Design, Synthesis and Biological Evaluation of Heterocyclic Molecules as Potential Anti-Cancer Agents

SUMMARY FOR THE DEGREE OF

DOCTOR OF PHILOSOPHY

In

Pharmaceutical Sciences

Candidate:

Mr. Sachin B. Puri

Supervisor

Dr. Kapil Juvale

Shobhaben Pratapbhai Patel

School of Pharmacy and Technology Management

SVKM's Narsee Monjee Institute of Management Studies,

V.L. Mehta Road, Vile Parle (W),

Mumbai-400 056

2023

TABLE OF CONTENTS

Sr. No.	Contents	Page. No.
1	Introduction	1
2	Statement of problem	3
3	Overview of Literature	3
4	Rationale of the study	6
5	Objectives	7-8
6	Experimental work	8-65
7	Summary and Conclusion	65-68
8	Future perspective	69
9	References	69-76

1. Introduction

Cancer is one of the leading causes of mortality and morbidity worldwide. As per the statistics given by National Centre for Health Statistics (NCHS) in the year 2022, around 19.8 million patients affected by cancer were confirmed and about 0.61 million cancer casualties were registered considering the worldwide scenario [1].

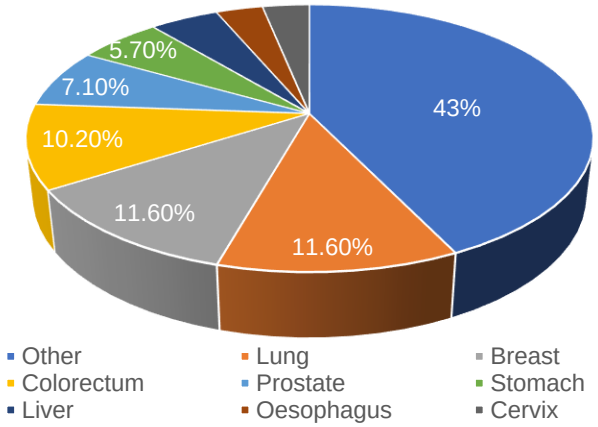

Figure 1: Cancer incidence statistics worldwide in 2022 by type of cancer

On the other hand, in economically underdeveloped or developing countries, mortality incidences are increasing for different cancers, the most fatal ones being lung and liver [2]. Chemotherapy and radiotherapy are the major non-invasive treatments available against cancer, but unfortunately success of these therapies largely depends upon occurrence of multidrug resistance (MDR) in tumor cells. A variety of pathways have been recognised as contributing factors to the formation of multidrug resistance (MDR) in cancer [3]. These include drug target loss, increased DNA repair mechanisms, decreased drug absorption, and increased drug efflux due to overexpression of ATP binding cassette (ABC) transporters. Aside from this, one of the key MDR mechanisms newly recognised in solid tumors is altered metabolism, particularly at the cellular glycolytic level [4].

ATP is an energy source enabling cell survival. In dividing healthy cells, ATPs are generated by oxidative phosphorylation (OXPHOS), producing around 36 mole of ATP per mole of glucose. Only under oxygen deficiency, the glycolysis proceeds through lactate formation, producing only 2 mole of ATP per mole of glucose. Cancer cells, in contrast do not utilize OXPHOS even in presence of oxygen. Instead, they utilize aerobic glycolysis involving lactate formation for producing 2 mole of ATP per mole of glucose. This phenomenon is also known as 'Warburg effect', the hallmark of rapidly multiplying cancer cells, wherein there is increased glycolysis forming large amounts of lactate even in presence of oxygen [5]. Because aerobic glycolysis produces less ATP, cancer cells require a considerable amount of glucose to survive and proliferate. It has been shown that malignant tumors are heterogeneous in nature i.e. they contain normoxic and hypoxic regions. Such hypoxic cells undergo glycolytic switch wherein glycolysis is uncoupled from the mitochondrial respiration. These cells show high expression of hypoxia inducible factor 1 (HIF-1), which in turn induces expression of glucose transporter 1 (GLUT1) protein. GLUT1 is responsible for the uptake of the glucose which is later converted to pyruvate, and ultimately to lactate and H^+ through glycolytic pathways [6].

The lactate and H^+ hence synthesized are effluxed through monocarboxylate transporter 4 (MCT4) overexpressed in hypoxic cells. This effluxed lactate is then captured by normoxic tumor cells with the help of overexpressed monocarboxylate transporter 1 (MCT1) and is reconverted to pyruvate using lactate dehydrogenase. The pyruvate formed is then used for mitochondrial OXPHOS to generate ATP i.e., reverse-Warburg effect [7]. Until now, 14 MCTs have been reported, amongst which only MCT1 to MCT4 transport monocarboxylates such as lactate, pyruvate and ketone bodies [8]. Out of these

four isoforms MCT1 and MCT4 are the most relevant for cancer progreesion and hence are the targets of interest.

2. Statement of problem

In the last few decades, substantial development has been made in identification of advanced anticancer agents. This advancement can be attributed to better understanding of targets, which has led to the identification of targeted therapies. Unfortunately, the older chemotherapeutic agents and newer drug are constantly facing a challenge of failure due to multifold reasons. Among these, the emergence of MDR is the main cause for non-responsiveness of chemotherapeutic agents. Apart from this, severe side effects make usefulness of such anticancer diminished. Hence, there is constant need to identify newer and safer anticancer agents having new targets. This will help in fulfilling the continuous need for better therapeutic agents with lesser side effects.

3. Overview of Literature

Lactate transporters MCT1 and MCT4 are overexpressed in solid tumors, and they work together to drive the lactate shuttle in tumors. Overexpression of MCT1 is found in variety of cancers including head and neck cancer, breast cancer, colon cancer and lung cancer. When the MCT1 in the aerobic cells is blocked, lactate transport in the tumor cells comes to a halt. To compensate for this lack of lactate, the aerobic cells must now import glucose, which otherwise they didn't need. This is because in the normal condition, hypoxic region would import glucose and produce lactate as source of energy for the aerobic region. This disturbs the symbiosis established between normoxic and hypoxic tumor regions, forcing the aerobic cells to take up more glucose from nearby blood vessels. When glucose is

exhausted in the aerobic region itself, the hypoxic region does not receive its one and only energy source i.e., glucose. This leads to apoptosis induction in the hypoxic cells as a result of glucose starvation. Hence, inhibition of MCT1 present on the normoxic cells indirectly kill the hypoxic cells, which are otherwise resistant to conventional chemotherapeutic methods and contribute to tumor relapse [9,10]. This phenomenon makes MCT1 an attractive target for cancer therapy; as after killing the hypoxic cells only the more manageable aerobic cells are left, which can be treated using standard chemotherapeutic methods or radiotherapy [11] .

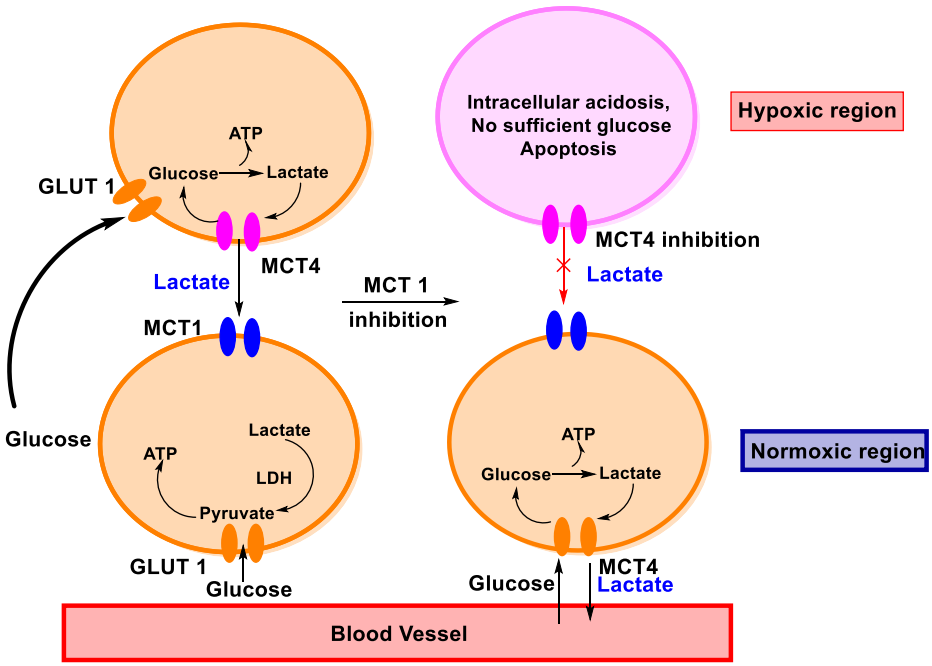

Figure 2: Mechanism of Monocarboxylate transporters

Until now, a few inhibitors of MCT1 reported in the literature which include molecules having scaffolds such as flavonoids, coumarins, uracil and cyanoacetic acid derivatives which are summarized in **figure 3.** After the discovery that lactic acid efflux from cells is carrier-mediated, it was postulated that inhibition of this efflux could be a potential target

for chemotherapy [20,21]. The lack of specific and potent inhibitors of these transporters slowed down the study of potential of MCTs as target. The first inhibitor to confirm the postulation was α-cyano-4-hydroxycinnamate [22], which lacks the specificity amongst MCTs. Several naturally occurring flavonoids have been reported to be inhibitors of MCT1, where naringenin and silybin particularly exhibited strong inhibitory effect with lower IC_{50} values [23]. Another naturally occurring flavonoid quercetin was also shown to affect cell proliferation and apoptosis in bladder cancer by targeting MCT1 which lead to alteration in the tumor microenvironment [24].

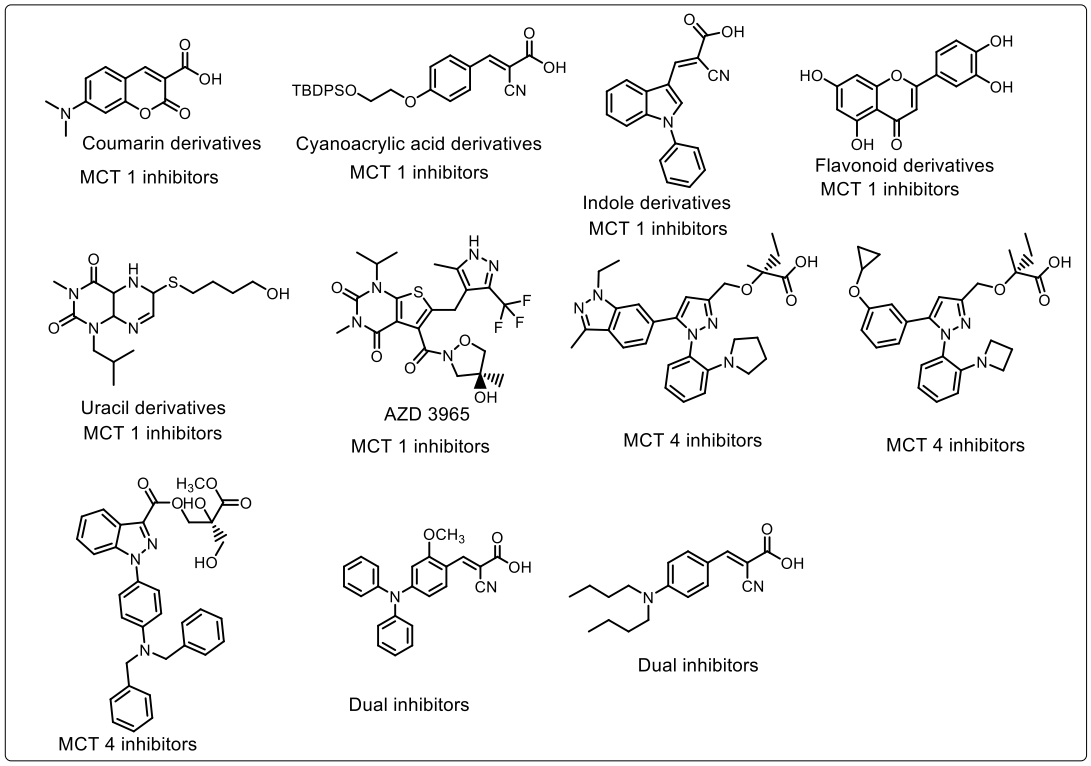

Figure 3: Important MCT1 and MCT4 inhibitors reported in literature

MCT1 inhibitor developed by Astra Zeneca (AZD 3965) was the first, potent and selective inhibitor of MCT1. The preclinical data showed that AZD3965 was able to inhibit MCT1 at

10µM concentration with no effect on the MCT4. This compound is currently undergoing clinical trials for patients with advanced solid tumors (in which treatment failure due to hypoxic tumor is predominantly seen). AZD3965 has been investigated for its effect in small cell lung cancer [25] and irradiating cancer stem cells [26].

Recently, Draoui *et al* reported several 3-carboxycoumarins to be potent inhibitors of MCT1 and MCT4 proteins. In this study 7-alkylamino 3-carboxycoumarins were found to be the most potent compounds amongst studied analogues [27]. Very recently in 2016 Lee et al, reported the potential of MCT4 inhibition for treating metastatic gastric cancer. It was also reported that in comparison to MCT1 and MCT 2, expression levels of MCT4 were significantly high in malignant cells [28]. Choi *et al* have also put forward the potential of MCT4 as a novel and potential target for the therapy for advanced prostate cancer in their report in 2016 [29].

Research in the field of MCTs inhibitors as potential targets of solid cancer is still in nascent phase and there is a need for identification of new potent inhibitors which can foster the development of new therapeutics to treat the cancer.

4. Rationale of the study

Due to the emergence of MDR in cancer there is a need to identify newer anticancer agents having novel targets. MCTs are such new targets which have been recently recognized for their potential to treat cancer. Hypoxia and increased glycolysis are important hallmarks of cancer. One of the main hurdles in chemotherapy and radiotherapy success is the occurrence of MDR. With the understanding of role of hypoxia, altered metabolism and the lactate shuttle mechanism (especially in solid tumor cells) in cancer

cells and involvement of MCT1 and MCT4, new therapeutics could be developed. Suppressing the lactate flux with small molecules decreases the chances of development of drug resistance and consequent relapse. More recently, the lactate transporters MCT1 and MCT4, majorly expressed in tumor, have become leading targets under investigations. Moreover, a MCT1 inhibitor AZD3965 has already reached clinical stage. Although several MCT 1 inhibitors have been identified, MCT 4 inhibitors are lagging in this regard. Most of the MCT inhibitors identified until now are either selective towards MCT1 or MCT4. Dual inhibition of MCT1 and MCT4 would be advantageous as most of the tumors express both these transporters and if any one of them remains uninhibited could work in favor of the tumor growth. In the proposed work, the initial set of potential inhibitors was designed, synthesized, and screened for effectiveness. Based on the initial results obtained further potential targets were explored to find potent, selective and non-toxic inhibitors of MCT1 and / or MCT4.

5. Objectives

Objective of the current project are as under:

1. Knowledge based design of new anticancer agents with the help of *in silico* studies.
2. Synthesis and purification of molecules selected from *in silico* studies
3. Characterization of synthesized molecule using LCMS, HPLC, NMR, and FTIR
4. Biological evaluation of synthesized molecules by *in vitro* assays to determine effectiveness using different cancer cell lines.

5. Determination of intrinsic cytotoxicity (safety) of target molecules using healthy (non-cancer) cells.
6. Prediction of Structure Activity Relationship (SAR) based on biological activity

6. Experimental work

6.1. Knowledge based design of new anticancer agents with the help of *in silico* studies

Initially, target molecules for MCT1 and MCT4 were designed based on the previously reported scaffolds (**Figure 4**). It includes coumarin, flavonoids, indole, and indazole. Due to the lack of availability of a large pool of known inhibitors for MCT1 and MCT4, the initial design of small molecules was limited to the known scaffolds. Here we made the changes in the substitution pattern in the flavonoids, coumarins, and quinazolines. A library of these designed molecules will then be screened *in-silico* by molecular docking studies. The first modification was made in the free carboxyl group which was present in most of the known compounds by replacement with esters and amides. We also studied the effect of substitution on the aromatic rings present in these analogs. A total of 68 target molecules were synthesized in initial phase, which belongs to scaffold such as coumarin, flavonoids, quinazoline, N-substituted benzylated indole and indazole cyanoacrylate derivatives. Results obtained from initial screening indicated that none of the compounds showed substantial activity against MCT1 and MCT4 even at 25 µM concentration when compared with standard MCT1 inhibitors **CHC** or **UK-5099**. Based on this observation selection of different target molecules was carried out. The final target scaffold selected for further development includes indazole-3-carboxamide derivatives

linked with N-phenylacetamide or N-phenylpropanamide linker and indole cyanoacrylate derivatives linked with N-phenylacetamide based scaffold [30].

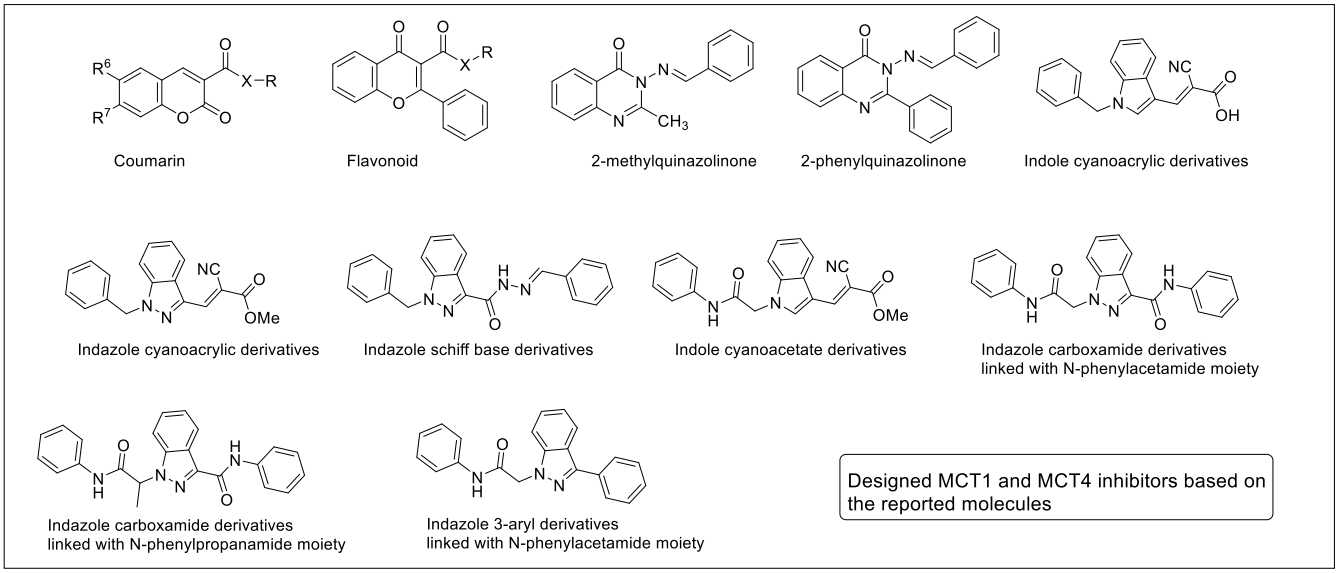
Coumarin
Flavonoid
2-methylquinazolinone
2-phenylquinazolinone
Indole cyanoacrylic derivatives
Indazole cyanoacrylic derivatives
Indazole schiff base derivatives
Indole cyanoacetate derivatives
Indazole carboxamide derivatives linked with N-phenylacetamide moiety
Indazole carboxamide derivatives linked with N-phenylpropanamide moiety
Indazole 3-aryl derivatives linked with N-phenylacetamide moiety
Designed MCT1 and MCT4 inhibitors based on the reported molecules

Figure 4: Design of target molecules based on reported scaffold.

6.1.1. Molecular docking

The protein databank entry 7CKR provides Cryo-EM structure of the human MCT1/Basigin-2 complex co-crystallised with anti-cancer drug candidate BAY-8002 in the outward-open conformation. The retrieved protein structure was prepared using the protein preparation wizard panel. Protein preparation was done by using prime. In this process, missing hydrogens were added, bond ordering was allocated, disulfide bonds were formed, and missing side chains and loops were substituted. In the last refinement stage, the OPLS3 force field was employed to accomplish complete energetic optimization, with the RMSD of heavy atoms set to 0.3 Å. Designed structures were prepared using the LigPrep module to achieve low energy 3D structures with suitable chiralities. The ionization state of each ligand structure was produced at a physiological

pH of 7.2 ± 0.2. The grid file for molecular docking was prepared by selecting co-crystallized ligand BAY-8002 using glide module. Glide computes a default center and size for the area for which grids will be generated depending on the ligand's location and size. Finally, the molecular docking investigation was carried out utilizing Schrodinger's glide, which included loading the prepared ligands and receptor grid file into Maestro's workspace and docking the ligands into the receptor binding pocket using standard precision (SP) docking method. Molecular docking results of selected designed molecules are shown in **figure 5**.

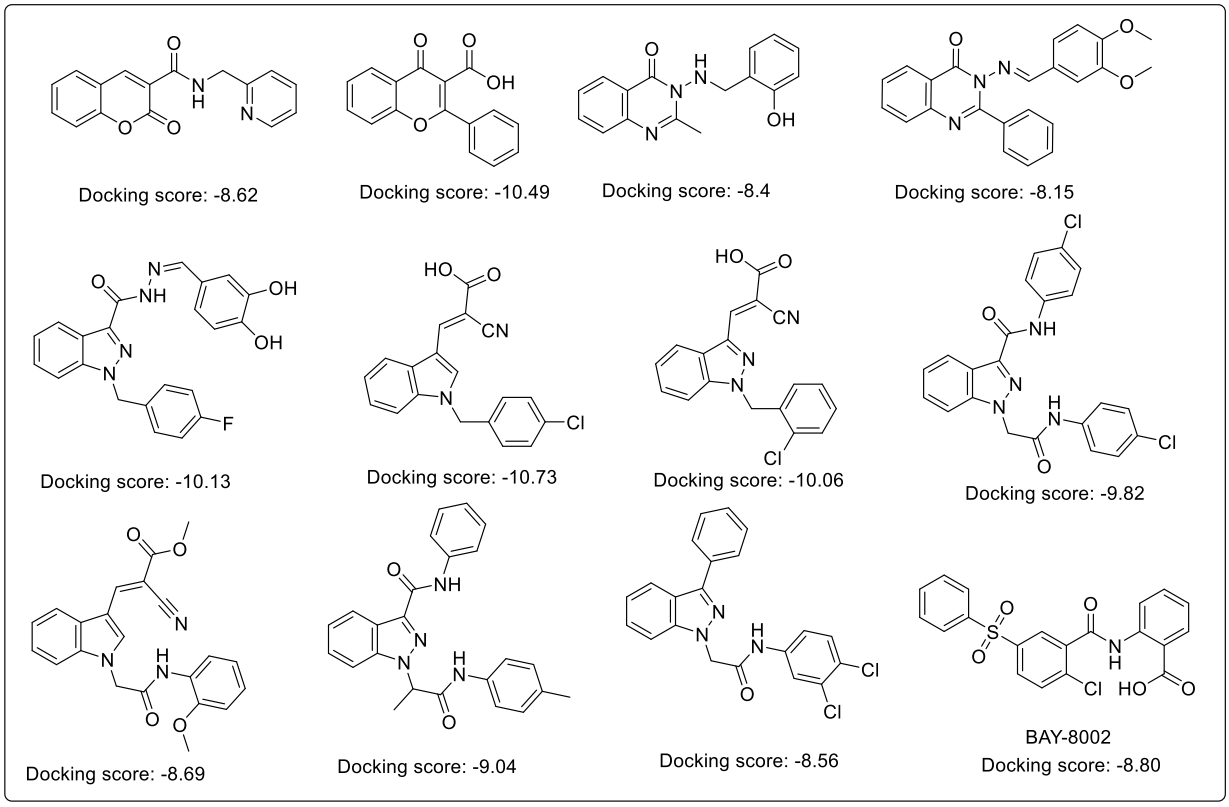

Figure 5 : Molecular docking results of designed molecules

6.2. Chemistry

6.2.1. Synthesis of coumarin derivatives (6-15)

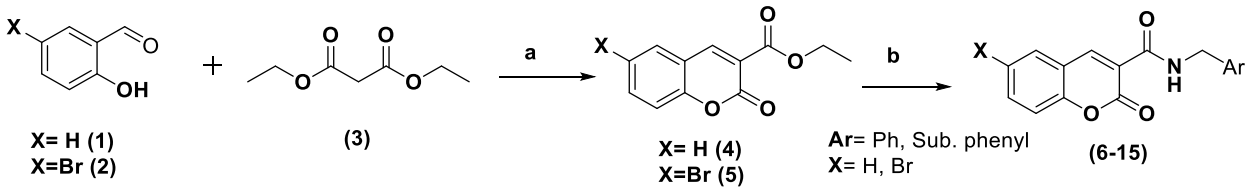

Reagent and conditions: a) Piperidine (1.1eq), cat. acetic acid, ethanol, 90°C, 30 min,
b) Substituted benzylamine (1.1 eq), ethanol, reflux, 16 hrs.

Scheme 1: Synthesis of coumarin derivatives

General Procedure

Step 1: General procedure for synthesis of ethyl 2-oxo-2H-chromene-3-carboxylate **(4** and **5)**

Coumarin esters **(4)** and **(5)** were synthesized by refluxing salicylaldehyde **(1)** or 5-bromosalicylaldehyde **(2)** (1eq) with diethyl malonate **(3)** (1.1eq) in presence of the catalytic amount of piperidine (1.1 eq) and acetic acid in ethanol for 30 min. Then reaction content was evaporated under vacuum to get the residue, the obtained product was recrystallized by using 70% alcohol to yield ethyl 2-oxo-2H-chromene-3-carboxylate **(4)** and ethyl 6-bromo-2-oxo-2H-chromene-3-carboxylate **(5).**

Step 2: General procedure for synthesis of N-benzyl-2-oxo-2H-chromene-3-carboxamide derivatives (6-15)

To a well-stirred solution of **(4)** or **(5**) (1 eq) in ethanol, equivalent amount of substituted benzyl amine (1 eq) was added. Then the resulting reaction mixture was allowed to reflux overnight at 80°C. Then reaction mixture was allowed to cool at 0˚C for 30 minutes. The solid precipitate was filtered under suction, and dried to get moderate to good yield of N-benzyl-2-oxo-2H-chromene-3-carboxamide derivatives **(6-15).**

6.2.2. Synthesis of flavonoid derivatives (29-34)

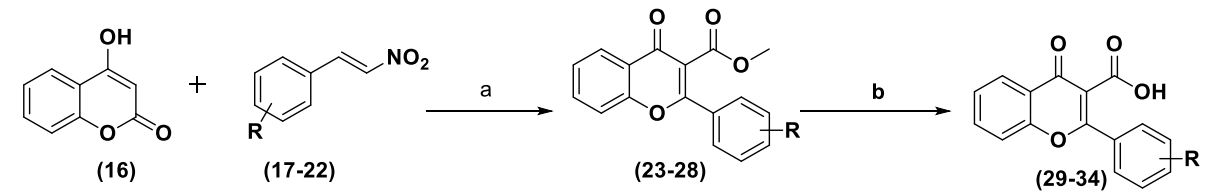

R= 17: 3,4-dimethoxy, **18:** 4-methyl, **19:** H **20:** 4-methoxy, **21:**4-chloro, **22:** 4-hydroxy

R= 23: 3,4-dimethoxy, **24:** 4-methyl, **25:** H **26:** 4-methoxy, **27:**4-chloro, **28:** 4-hydroxy

R= 29: 3,4-dimethoxy, **30:** 4-methyl, **31:** H **32:** 4-methoxy, **33:**4-chloro, **34:** 4-hydroxy

Reagent and conditions: a) DMAP (1.5eq), Methanol, 80°C, 3-5 hrs, b) lithium hydroxide (1.1 eq), THF: water (9:1), R.T, 16 hrs.

Scheme 2: Synthesis of flavonoid derivatives

***Step 1: General procedure for synthesis of methyl 4-oxo-2-phenyl-4H-chromene-3-carboxylate derivatives* (23-28)**

To a well-stirred solution of 4-hydroxycoumarin **(16)** (1 eq), substituted (E)-(2-nitrovinyl) benzene **(17-22)** (1 eq), in methanol (4 eq), 4-DMAP (1.5 eq) was added. The reaction content was refluxed for 3-5 hr. After completion of reaction as confirmed by TLC using 70% ethyl acetate in hexane as solvent, the content was evaporated under vacuum. The obtained product was further purified by column chromatography using 10-20% ethyl acetate in hexane as mobile phase to obtain target derivatives **(23-28)**.

Step 2: General procedure for synthesis of 4-oxo-2-phenyl-4H-chromene-3-carboxylic acid derivatives (29-34)

To a solution of ester derivatives **(23-28)** (1 eq) in THF: water (9:1), lithium hydroxide (1.1eq) was added at 0°C portion wise and stirred for 16 hr at room temperature. After completion of reaction, the excess solvent was evaporated under vacuum to obtain the crude. The crude was diluted with 2N HCl to get target derivatives with moderate to good yield.

6.2.3. Synthesis of 2-methylquinazoline derivatives (38-47 and 48-52) [31]

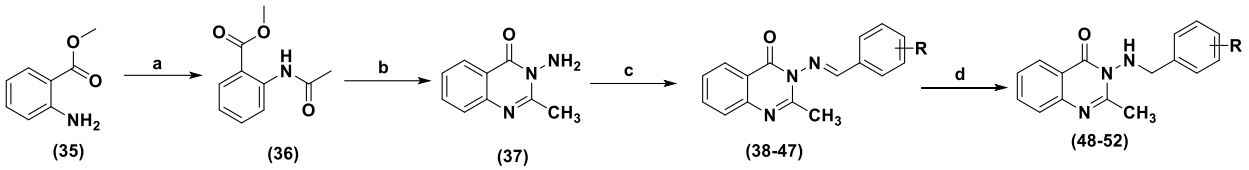

R: H, 4-Cl, 4-CH_3, 2-F, 4-CN, 3,4- OCH_3, 4-Br, 2-OH, etc

Reagent and conditions: a) acetic anhydride, reflux, 30 min.
b) $NH_2NH_2.4H_2O$ (10eq), ethanol, reflux, 1.5 hr.
c) Substituted benzaldehyde (1.1 eq), cat. acetic acid, ethanol, reflux, 16hr.
d) NaBH4 ,0°C-R.T, 3-5 hrs.

Scheme 3: Synthesis of 2-methylquinazoline derivatives

Step 1: General procedure for synthesis of methyl 2-acetamidobenzoate (36)

To a stirred solution of methyl anthranilate **(35)** (1 eq), and acetic anhydride was refluxed for 30 min, and the progress of the reaction was monitored by TLC using 30% ethyl acetate in hexane as a mobile phase. After completion of the reaction, the resulting reaction mixture was poured into cold water containing few drops of pyridine and stirred until oily substance solidified. The solid formed was filtered off and dried to furnish compound **36** with **95 %** yield.

Step 2: General procedure for synthesis of 3-amino-2-methylquinazolin-4(3H)-one (37)

To a stirred solution of **36** (1 eq), and hydrazine hydrate (10 eq) in ethanol was refluxed for 1.5 hr and the progress of the reaction was monitored by TLC using 30% ethyl acetate in hexane as a mobile phase. Then the resulting reaction mixture was poured into ice cold water. The precipitate was filtered off and dried to afford compound **37** with **68%** yield**.**

Step 3: General procedure for synthesis of (E)-3-(benzylidene amino)-2-methylquinazolin-4(3H)-one derivatives (38-47)

To a mixture of **37** (1 eq) and substituted aldehyde (1.1eq) in ethanol was allowed to stir at room temperature for 10 min and to this mixture catalytic amount of glacial acetic acid was added and reaction was refluxed for 15-16 hr. After completion of the reaction as confirmed by TLC using 30 % ethyl acetate in hexane as a mobile phase, resulting reaction mixture was cooled. Resulting solid product was separated by filtration, and dried, to afford desired compound with **54-58%** yield.

Step 4: General procedure for synthesis of 3-(benzylamino)-2-methylquinazolin-4(3H)-one (48-52)

To a stirred solution of imines **(38-47)** (1 eq), in methanol was added $NaBH_4$ at 0°C and the reaction mixture was allowed to stir for 3-5 hr at room temperature. After completion of reaction as confirmed by TLC using 30 % ethyl acetate in hexane as solvent system, the reaction content was concentrated the under vacuum, solid formed was filtered off, washed with cold water to obtain desired compound with **50-55%** yield.

6.2.4. Synthesis of 2-phenylquinazoline derivatives (56-65)

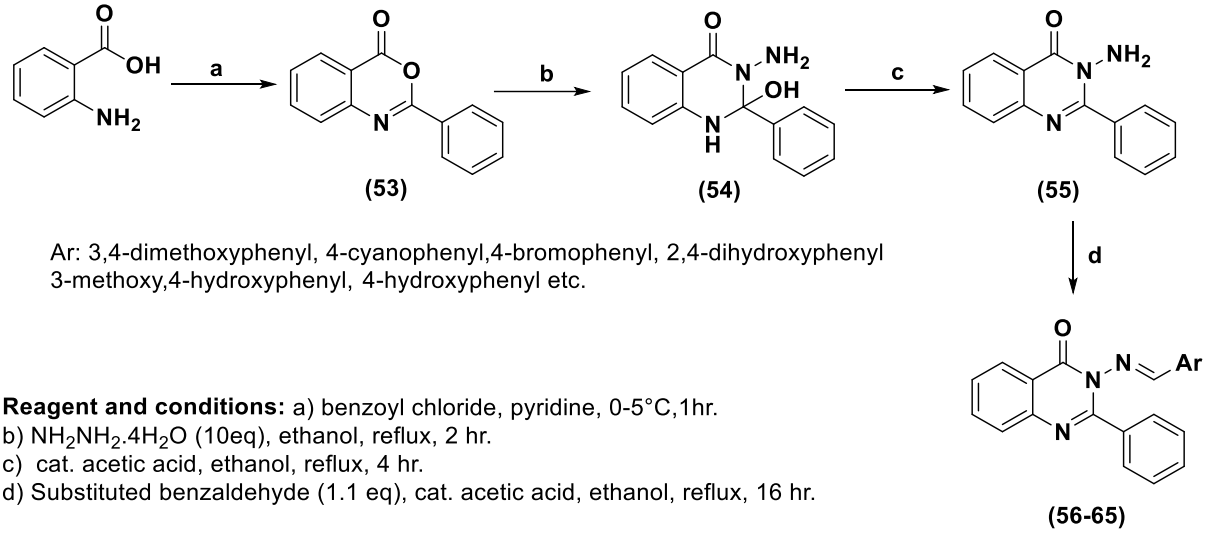

Scheme 4: Synthesis of 2-phenylquinazoline derivatives

Step1: Synthesis of 2-phenyl-4H-benzo[d][1,3] oxazin-4-one (53)

A solution of anthranilic acid (1 eq) in pyridine was prepared and stirred vigorously. Slowly benzoyl chloride (1.5 eq) was added to the solution at 0^{o}C. The resulting mixture was then allowed to stir at room temperature for 1 hr. The progress of reaction was monitored by TLC with mobile phase consisting of 20% ethyl acetate in hexane. After completion of reaction, the reaction mixture was diluted with saturated $NaHCO_3$ solution and mixture was allowed to stir for additional 30 min. The resulting solid product was separated by suction, and residue was washed with water and dried to yield the desired compound **(Yield 80%).**

Step 2: Synthesis of 3-amino-2-hydroxy-2-phenyl-2,3-dihydroquinazolin-4(1H)-one (54)

To a well-stirred solution of compound **53** (1 eq) in absolute ethanol was added hydrazine hydrate 99% (1.2 eq) slowly at 0^{o}C, and reaction mixture was allowed to reflux for 2 hr. The progress of reaction was monitored by TLC with mobile phase consisting of 20% ethyl acetate in hexane. Then reaction content was concentrated under vacuum and dried. Obtained intermediate was taken forward for next reaction without further purification **(Yield 70%).**

Step 3: Synthesis of 3-amino-2-phenyl-1H-quinazolin-4-one (55)

To a well-stirred solution of compound **54** (1 eq) in ethanol was added glacial acetic acid (2 eq) and the reaction mixture was refluxed for 4-5 hr. The progress of reaction was

monitored by TLC with mobile phase consisting of 70% ethyl acetate in hexane. After completion of reaction, mixture was concentrated under vacuum to obtained crude, and crude was transferred into ice cold water to get solid. The obtained intermediate was used in next step without further purification (**Yield 65 %).**

Step 4: Synthesis of (E)-3-(benzylidene amino)-2-phenylquinazolin-4(3H)-one derivatives (56-65)

To a well-stirred solution of compound **55** (1 eq) and substituted benzaldehyde (1eq) in ethanol, was added catalytic amount of glacial acetic acid and the reaction mixture were refluxed for 16 hr. The reaction was monitored by TLC with mobile phase consisting of 70% ethyl acetate in hexane. Then excess of ethanol was evaporated under vacuum to get residue. Then residue was washed with ice-cold water to get solid product, which was further purified by column chromatography by using 20% ethyl acetate as eluent. **(Yield 80%).**

6.2.5. Synthesis of (E)-1-benzyl-N'-benzylidene-1H-indazole-3-carbohydrazide derivatives (73-83)

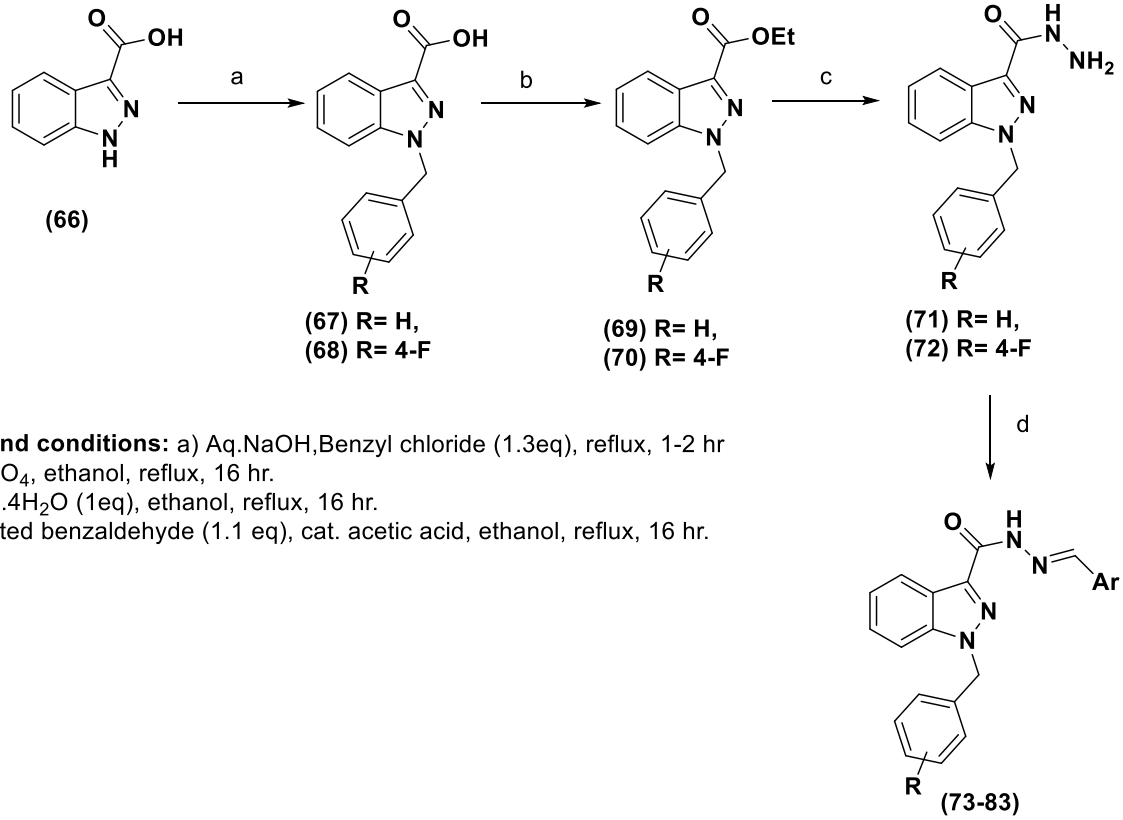

Reagent and conditions: a) Aq.NaOH,Benzyl chloride (1.3eq), reflux, 1-2 hr
b) Cat.H_2SO_4, ethanol, reflux, 16 hr.
c) $NH_2NH_2.4H_2O$ (1eq), ethanol, reflux, 16 hr.
d) Substituted benzaldehyde (1.1 eq), cat. acetic acid, ethanol, reflux, 16 hr.

Scheme 5: Synthesis of (E)-1-benzyl-N'-benzylidene-1H-indazole-3-carbohydrazide

Step 1: Synthesis of Substituted 1-benzyl-1H-indazole-3-carboxylic acid (67-68)

To a stirred solution of indazole-3-carboxylic acid **66** (1 eq) in a solution of equivalent amount of NaOH in water, while heating on water bath substituted benzyl chloride (1.3 eq) was added with stirring. After heating for 2 more hours the solution was cooled and acidified with dilute hydrochloric acid to get crude 1-benzyl-1H-indazole-3-carboxylic acid derivatives. Precipitated product was filtered and recrystallized from 30% ethanol:water system. (**Yield 90%**).

Step 2: Synthesis of ethyl-1-benzyl-1H-indazole-3-carboxylic acid (69-70) [32]

A solution of 1-benzyl indazole-3-carboxylic acid **67-68** (1 eq) was prepared in ethanol and stirred. A catalytic amount of sulfuric acid and the reaction mixture was heated under reflux for 16 hr. The progress of the reaction was monitored using TLC. Once the reaction was complete, the mixture was evaporated and resulting crude product was purified by column chromatography (**Yield 70%**)

Step 3: Synthesis of (1-benzyl-1H-indazol-3-yl)(1λ^4-diazaneyl)methadone (71-72).

To a well stirred solution of **69-70** in ethanol was added hydrazine monohydrate (1 eq) slowly at 0°C, and the reaction mixture was allowed to reflux for 16 hr. After completion of reaction as indicated by TLC, the reaction mixture was evaporated to get solid precipitates, which was recrystallised with ethanol to afford **71-72.** (**Yield 73%**)

Step 4: *Synthesis of substituted (E)-1-benzyl-N'-benzylidene-1H-indazole-3 carbohydrazide (73-83)*

To a stirred solution of (1-benzyl-1H-indazol-3-yl)(1λ^4-diazaneyl)methadone **71-72** (1 eq) and substituted benzaldehyde (1 eq) in ethanol was added catalytic amount of glacial acetic acid and allowed reaction mixture was heated under reflux for 15-16 hr. Once the reaction was complete as indicated by TLC, reaction content was cooled, solid formed was filtered off, washed with water and dried, to afford desired compound **54-58%** yield.

6.2.6. Synthesis of E)-3-(1-benzyl-1H-indol-3-yl)-2-cyanoacrylic acid derivatives 93-99 and 100-102)

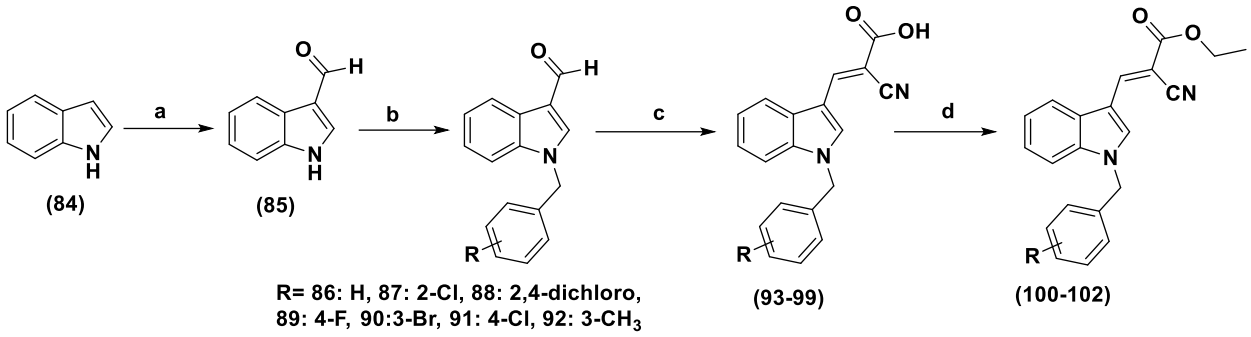

Reagent and conditions: a) *N,N*-dimethylformamide, $POCl_3$ (2 eq), reflux, 1-2 hr.
b) Sub. benzyl bromide (1.1 eq), NaH (1.5eq), DMF, 2-3 hr.
c) Cyanoacetic acid (1 eq), cat.piperidine, acetonitrile, reflux, 16 hr.
d) Methyl cyanoacetate (1.1 eq), cat. piperidine, ethanol, 1 hr.

Scheme 6: Synthesis of (E)-3-(1-benzyl-1H-indol-3-yl)-2-cyanoacrylic acid derivatives

Step 1: Synthesis of 1H-indole-3-carbaldehyde (85)

To a cooled solution of DMF, $POCl_3$ (2 eq) was added. The resulting reaction mixture was stirred for 30 min at 0°C. Then, a solution of indole (1 eq) in a small amount of DMF was added dropwise to the mixture over a period of 20 min. The mixture was stirred at room temperature for 2 hr. Next, a small amount of crushed ice was added, and mixture was neutralized using NaOH. The resulting precipitate was filtered, washed with water, and dried to obtain the desired compound (**Yield ~90%).**

Step 2: Synthesis of 1-benzyl-1H-indole-3-carbaldehyde (86-92)

In DMF, a solution of indole-3-carboxaldehyde derivative **85** (1 eq) was prepared. Sodium hydride (NaH) (1.5 eq) was added to the solution at 0°C, and the reaction mixture was stirred for 20 min at same temperature. Subsequently, a substituted benzyl bromide (1.1 eq) was added. The reaction mixture was stirred at room temperature for 4-6 hr, and the progress of reaction was monitored using TLC. Once the reaction was complete, ice cold

water was added. The resulting precipitate was filtered and then purified by column chromatography with a solvent system of 20% ethyl acetate in hexane. This process yielded N- alkylated indole-3-carboxaldehyde derivative **69-75 (Yield 72%).**

Step 3: Synthesis of (E)-3-(1-benzyl-1H-indol-3-yl)-2-cyanoacrylic acid (93-99)

To a well stirred solution of 1-benzyl-1H-indole-3-carbaldehyde **86-92** (1 eq) in acetonitrile was added cyanoacetic acid (1 eq), and few drops of piperidine, then reaction mixture was refluxed for 6-7 hr. After completion of the reaction as indicated by TLC, reaction mixture was acidified with 3N HCl. The solid formed was filtered off, dried, and recrystallized from 70% ethanol to furnish the final product ***93-99*** **(Yield 70%).**

Step 4: Synthesis of ethyl (E)-3-(1-benzyl-1H-indol-3-yl)-2-cyanoacrylate via Knoevenagel condensation (100-102)

1-Benzyl-1H-indole-3-carbaldehyde (1eq) and methyl cyanoacetate (1eq) were mixed with ethanol (10 mL), and to the mixture a few drops of piperidine was added and the reaction mixture was allowed to stir at room temperature for 6-8 hr. After completion of the reaction the reaction content was concentrated under reduced pressure, and the residue was acidified with 3N HCl. The obtained solid was filtered off, dried, and recrystallized from 70% ethanol to furnish the final product **100-102 (Yield 70-80%).**

6.2.7. Synthesis of (E)-3-(1-benzyl-1H-indazol-3-yl)-2-cyanoacrylic acid derivatives (96-102)

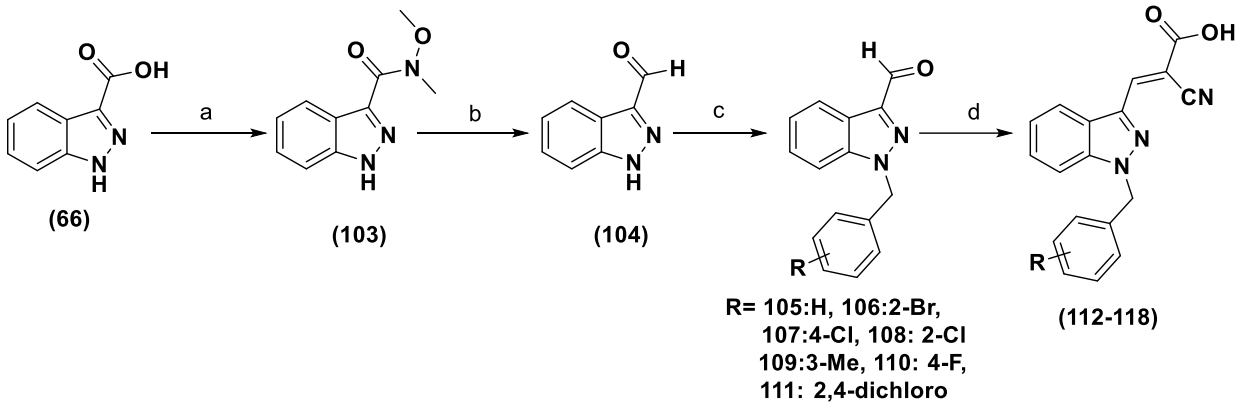

Reagent and conditions: a) *N,O*-dimethylhydroxylamine hydrochloride (1.1 eq), EDC.HCl (2 eq), Pyridine (4.2 eq), °C - R.T. 4 hr. b) $LiAlH_4$ (1.5 eq), THF, -15°C - 0°C. 4 hr . c) sub. benzyl bromide (1.1 eq), NaH (1.5 eq) ,DMF, 2-3 hr. d) cyanoacetic acid (1 eq), cat. piperidine, acetonitrile, reflux, 16 hr.

Scheme 7: Synthesis of (E)-3-(1-benzyl-1H-indazol-3-yl)-2-cyanoacrylic acid derivatives

Step 1: Synthesis of Weinreb amide (103) [33]

To a well-stirred solution of indazole 3-carboxylic acid **66** (1 eq) in THF was added N, O-dimethyl hydroxylamine hydrochloride portion wise (1.1 eq) at 0°C, followed by addition of pyridine (2.2 eq). Then reaction mixture was stirred for 1.5 h at 0°C and pyridine (2 eq) and EDC (2 eq) were added. The reaction mixture was stirred for 16 hr at room temperature. Once the reaction was completed as indicated by TLC, reaction mixture was evaporated under vacuum. Followed by crushed ice was added and the resulting precipitate was filtered and washed with cold water to obtain the desired product (**103**).

Step-2: Synthesis of 1H-indazole-3-carbaldehyde (104)

To a cooled solution of Weinreb amide (**103**) in THF was added Lithium aluminium hydride at -15°C (1.5 eq). The reaction mixture was allowed to stir at same temperature for 16hr. Reaction mixture was cooled at 0°C and neutralised with 2N HCl, the solid material was

filtered, and filtrate was extracted with ethyl acetate. The organic layer was passed over Na_2SO4 and evaporated under vacuum. The crude material was purified by flash chromatography using ethyl acetate: hexane (30:70) as mobile phase to obtain the desired indazole-3-aldehyde intermediate **(104).**

Step-3: Synthesis of 1-benzyl-1H-indazole-3-carbaldehyde derivatives (105-111)

To a well-stirred solution of indazole-3-aldehyde **104** (1eq) in dry DMF was added Sodium hydride (NaH) (1.5 eq) at 0°C and reaction mixture was stirred for 30 min at the same temperature. The appropriate amount of substituted benzyl bromide derivative (1.1 eq), was added to the above reaction mixture. The reaction mixture was stirred for additional 4-6 hr at room temperature. Once the reaction was completed as indicated by TLC, ice cold water was added slowly to the reaction mixture. The solid formed was filtered under suction, dried, and recrystallized from 70% ethanol to obtained N-alkylated indole-3-carboxaldehyde derivative (**105-111**).

Step 4: Synthesis of (E)-3-(1-benzyl-1H-indazol-3-yl)-2-cyanoacrylic acid (112-118)

1-Benzyl-1H-indole-3-carbaldehyde **105-111** (1 eq) and cyanoacetic acid (1 eq) were mixed with acetonitrile (10 mL), and to this mixture was added a few drops of piperidine. The reaction was refluxed for 7-8 hr. After completion of reaction as indicated by TLC, the reaction mixture containing acetonitrile was evaporated under reduced pressure, and the crude was acidified with 2N HCl. The obtained solid was filtered under suction, dried and recrystallized from 70% ethanol to furnish the desired product **(112-118).**

6.2.8. Synthesis of 1-(2-oxo-2-(phenylamino)ethyl)-N-phenyl-1H-indazole-3-carboxamide derivatives (122-157)

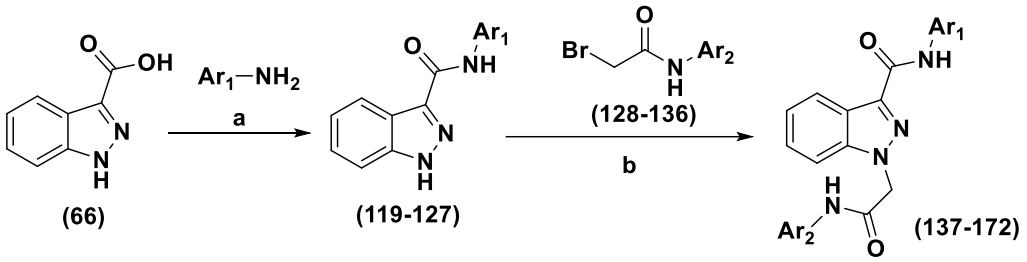

Ar_1= 4-chlorophenyl, 4-bromophenyl,3,4-difluorophenyl,3-methoxyphenyl, phenyl, 2-bromophenyl, 2-aminopyridine, 3-aminopyridine, 4-methoxyphenyl,
Ar_2 = 4-chlorophenyl, 4-methoxyphenyl, 2-chlorophenyl, 2-methoxyphenyl, 3-methoxyphenyl, 2,5-dichlorophenyl, 2,6-dichlorophenyl, 4-bromophenyl, 3,5-dichlorophenyl

Reagent and conditions: a) EDC.HCl (1.1 eq), HOBt (1.2 eq), substituted amine (1.1 eq) DMF, reflux, 2 hr. b) K_2CO_3 (3 eq), 2-bromo-N-phenylacetamide derivatives (1.3 eq) DMF, 3-4 hr

Scheme 8: Synthesis of 1-(2-oxo-2-(phenylamino) ethyl)-N-phenyl-1H-indazole-3-carboxamide derivatives

Step 1: Synthesis of N-phenyl-1H-indazole-3-carboxamide derivatives (119-127)

To a stirring solution of indazole 3-carboxylic acid **66** (1.0 eq) in DMF, was added HOBt (1.2 eq) and EDC. HCl (1.2 eq) subsequently. After stirring for 15 minutes, aniline (1.1 eq) was added dropwise, then the entire solution was refluxed at 90 °C for 2 hr. The completion of reaction was monitored using TLC. Subsequently, the solvent was removed under reduced pressure, and the remaining residue was washed with water and brine solution and extracted with ethyl acetate (3 × 30 mL). The combined organic layer was dried using anhydrous Na_2SO_4 and the solvent was evaporated under reduced pressure. The resulting crude solid was recrystallized from absolute ethanol to provide the desired product with moderate to good yield.

Step 2: Synthesis of N_1-alkylated 1H-indazole-3-carboxamide derivatives (137-172)

[34]

A solution of N-phenyl-1H-indazole-3-carboxamide derivative **119-127** (1 eq) in DMF (5 mL) was added potassium carbonate (3 eq) and the reaction mixture was stirred for 10 min at room temperature. To this 2-bromo-N-phenylacetamide **(128-136)** derivative (1.3 eq), was added. The reaction mixture was stirred for 4-6 hr at room temperature. The solvent was removed in pressure, ice-cold water was added. The formed precipitate was filtered off, dried and recrystallized from 95% ethanol to furnish N_1- alkylated 1H-indazole-3-carboxamide derivative.

6.2.9. Synthesis of methyl 2-cyano-3-(1-(2-oxo-2-(phenylamino) ethyl)-1H-indol-3-yl) acrylate derivatives (176-191) [21]

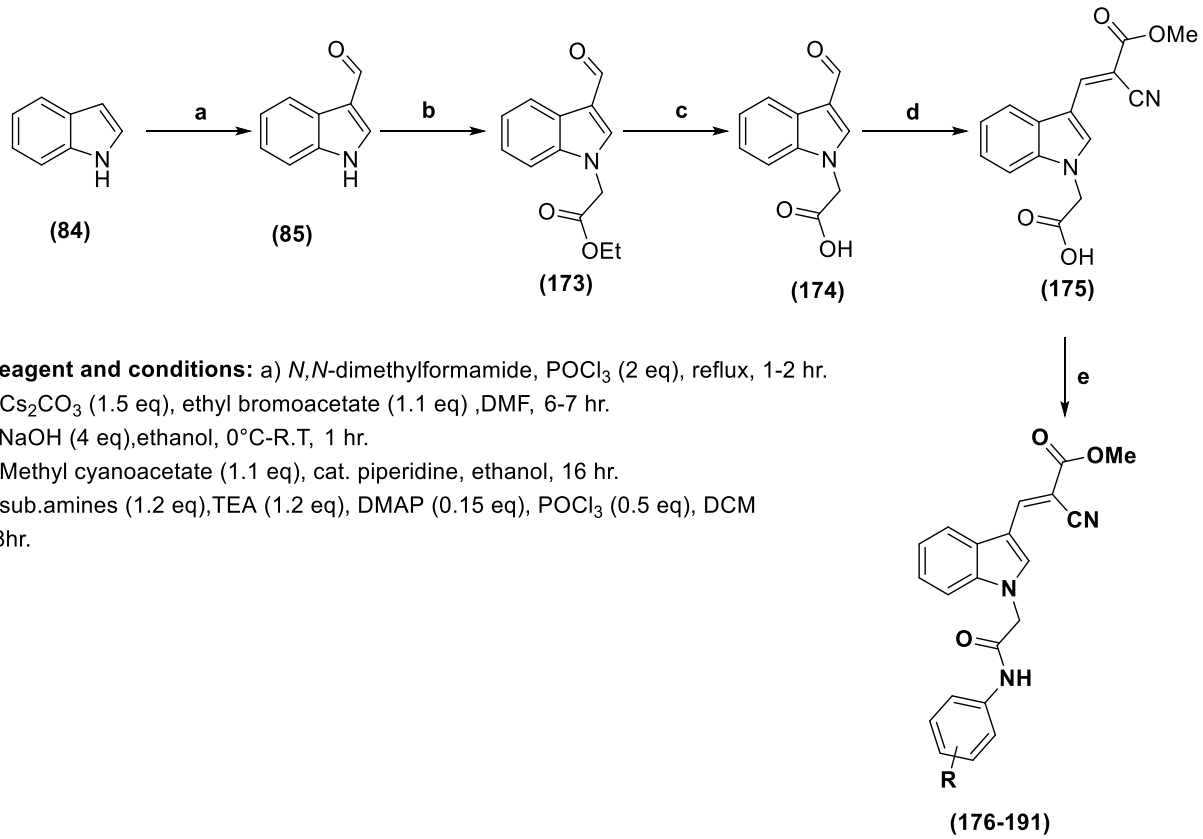

[a]**Reagent and conditions:** a) *N,N*-dimethylformamide, $POCl_3$ (2 eq), reflux, 1-2 hr.
b) Cs_2CO_3 (1.5 eq), ethyl bromoacetate (1.1 eq) ,DMF, 6-7 hr.
c) NaOH (4 eq),ethanol, 0°C-R.T, 1 hr.
d) Methyl cyanoacetate (1.1 eq), cat. piperidine, ethanol, 16 hr.
e) sub.amines (1.2 eq),TEA (1.2 eq), DMAP (0.15 eq), $POCl_3$ (0.5 eq), DCM 6-8hr.

Scheme 9: Synthesis of methyl 2-cyano-3-(1-(2-oxo-2-(phenylamino) ethyl)-1H-indol-3-yl) acrylate derivatives

Step1: Synthesis of 1H-indole-3-carbaldehyde (85)

DMF was cooled in an ice-salt bath and treated with phosphoryl chloride (2 eq). The resulting mixture was stirred for 20 min and added dropwise over 8 min to a similarly cooled solution of indole **84** (1eq) in *N*,*N*-dimethylformamide (25 mL) with stirring. The mixture was stirred further at room temperature for 2 hr followed by addition of small amount of crushed ice. The resulting mixture was basified to pH 14 with 5 M NaOH. After stirring at ambient temperature for 1 hr the precipitate was filtered, washed with water, and dried to give the compound (**Yield ~70%).**

Step 2: Synthesis of ethyl 2-(3-formyl-1H-indol-1-yl) acetate (173)

A solution of indole-3-carboxaldehyde derivative **85** (1 eq) in DMF (5 mL) was added cesium carbonate (Cs_2CO_3) (1.5 eq) and the reaction mixture was stirred for 10 min at room temperature. Then ethyl bromoacetate (1.1 eq), was added. The reaction mixture was stirred for 4-6 hr at room temperature followed by addition of ice-cold water. The formed precipitate was filtered off, dried, and recrystallized from 95% ethanol to furnish N-alkylated indole-3-carboxaldehyde derivative (**Yield ~ 86%).**

Step 3: Synthesis of 2-(3-formyl-1H-indol-1-yl) acetic acid (174)

To the solution of ethyl 2-(3-formyl-1H-indol-1-yl) acetate **173** NaOH solution (4 eq) in ethanol was added at room temperature under stirring. The stirring was continued till the starting material completely utilized (45-60 min). The resulting mixture was evaporated in under vacuum. The residue was acidified with 1M HCl, and the formed precipitate was filtered off, dried, and recrystallized from 95% ethanol to furnish desired acid **221** (**Yield ~ 70%).**

Step 4: Synthesis of (E)-2-(3-(2-cyano-3-methoxy-3-oxoprop-1-en-1-yl)-1H-indol-1-yl) acetic acid (175)

Compound **174** (1 eq) and methyl cyanoacetate (1 eq) were mixed with ethanol (10 mL), and to the mixture a few drops of piperidine were added. The mixture was stirred for 6-7 hr. The reaction mixture was concentrated under reduced pressure, and the residue was acidified with 2N HCl the formed precipitate was filtered off, dried and recrystallized from 95% ethanol to furnish the final product **175** (**Yield ~ 75%).**

Step 5: Synthesis of methyl (E)-2-cyano-3-(1-(2-oxo-2-(phenylamino)ethyl)-1H-indol-3-yl)acrylate (176-191)

To stirred solution of **175** (1 eq) in dichloromethane, substituted amine (1.2 eq) and triethylamine (1.2 eq) were added at 0°C under nitrogen and reaction mixture was allowed to stir for 20 min. Then DMAP (0.15 eq), and $POCl_3$ (0.5 eq) were added to the reaction mixture at 0°C. The resulting reaction mixture was stirred at 0°C for 15 min and then allowed to stir at room temperature for 6-8 hr. After completion of reaction as indicated by TLC, the resulting reaction mixture was poured into water (60 ml) and extracted with EtOAc (2 x 20 ml). The combined organic phase was dried over Na_2S0_4, filtered and concentrated under reduced pressure yielding compounds **176-191 (Yield ~ 80%).**

6.2.10. Synthesis of 1-(1-oxo-1-(phenylamino) propan-2-yl)-N-phenyl-1H indazole-3-carboxamide derivatives (197-209)

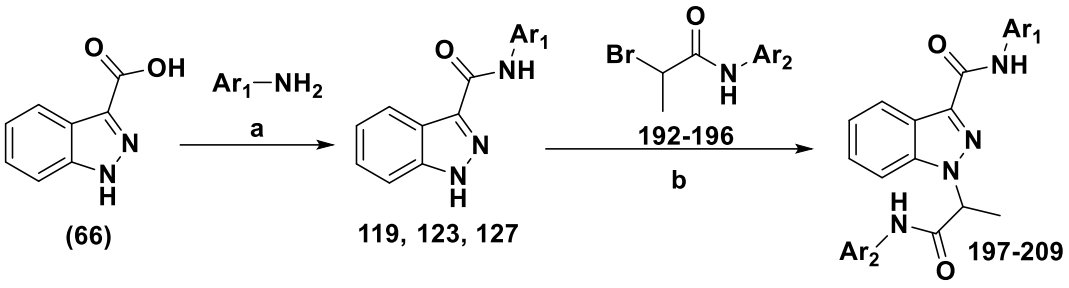

Ar_1= **119:** 4-chlorophenyl, **123:** phenyl, **127:** 4-methoxyphenyl,
Ar_2 = **192**: phenyl, **193**: 4-methylphenyl, **194**: 4-methoxyphenyl, **195**:2-methylphenyl, **196**: 4-fluorophenyl

Reagent and conditions: a) EDC.HCl (1.1 eq), HoBt (1.2 eq), substituted amine (1.1 eq) DMF, reflux, 2hr. b) K_2CO_3 (3 eq), 2-bromo-N-phenylacetamide derivatives (1.3 eq) DMF, 3-4 hr

Scheme 10: Synthesis of 1-(1-oxo-1-(phenylamino) propan-2-yl)-N-phenyl-1H-indazole-3-carboxamide derivatives

Step 1: Synthesis of N-phenyl-1H-indazole-3-carboxamide derivatives (119,123,127)

To a stirring solution of indazole 3-carboxylic acid **66** (1.0 eq) in DMF, was added HOBt (1.2 eq) and EDC. HCl (1.2 eq) subsequently. After stirring for 15 minutes, aniline (1.1 eq) was added dropwise, then the entire solution was refluxed at 90 °C for 2 hr. The completion of reaction was monitored using TLC. Subsequently, the solvent was removed under reduced pressure, and the remaining residue was washed with water and brine solution and extracted with ethyl acetate (3 × 30 mL). The combined organic layer was dried using anhydrous Na_2SO_4 and the solvent was evaporated under reduced pressure. The resulting crude solid was recrystallized from absolute ethanol to provide the desired product with moderate to good yield.

Step 2: Synthesis of N_1- alkylated 1H-indazole-3-carboxamide derivative (197-209)

In a solution of N-phenyl-1H-indazole-3-carboxamide derivative **119, 123, 127** (1 eq) in DMF (5 mL) potassium carbonate was added (1.5 eq) and the reaction mixture was stirred

for 10 min at room temperature. Then, 2-bromo-N-phenylpropanamide **(192-196)** derivative (1.3 eq), was added. The reaction was further stirred for 4-6 hr at room temperature. The solvent was removed under pressure, ice-cold water was added. The resulting precipitate was filtered off, dried and recrystallized from 95% ethanol to obtain the N_1- alkylated 1H-indazole-3-carboxamide derivative (**Yield ~70%).**

6.2.11. Synthesis of 1-(1-oxo-1-(phenylamino) propan-2-yl)-N-phenyl-1H-indazole-3-carboxamide derivatives (260-269)

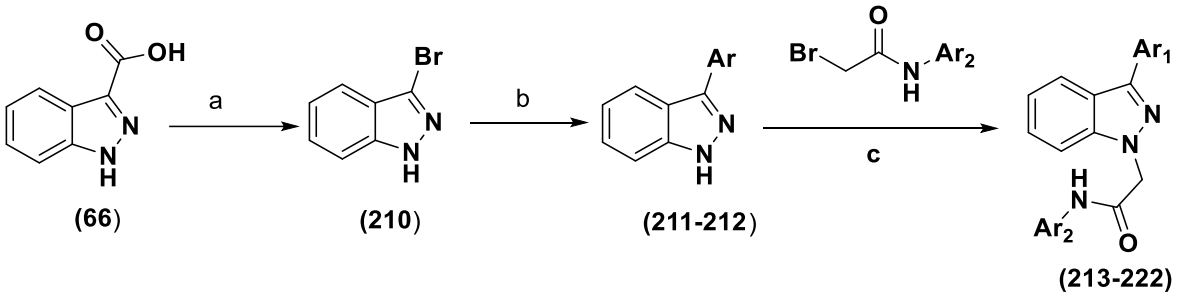

Ar_1= **199:** phenyl boronic acid, **200:**4-methylsulfonyl phenyl boronic acid
Ar_2 = phenyl, 2-methylphenyl, 4-methylphenyl, 4-methoxyphenyl, 4-fluorophenyl

[a]**Reagent and conditions:** a) NBS (1 eq) DMF, 0°C -R.T, 12 hr,
b) sub.boronic acid (1.2 eq) (Cs_2CO_3 (2.5 eq), Dioxane : water (3:1 eq), reflux, 16hr
c) K_2CO_3 (4 eq), 2-bromo-N-phenylacetamide derivatives (1.3 eq) DMF, 6-12 hr

Scheme 11: Synthesis of 1-(1-oxo-1-(phenylamino) propan-2-yl)-N-phenyl-1H-indazole-3-carboxamide derivatives

Step 1: Synthesis of 3-bromo-1H-indazole (210) [35]

A solution of 1H-indazole-3-carboxylic acid **(66)** (1 eq) in DMF was stirred at 0°C. N-bromo succinimide (1 eq) was added to the solution. The reaction mixture was allowed to stir at room temperature for 12 to 16 hr. Once the reaction was complete (as confirmed by TLC analysis), the reaction mixture was poured into ice cold water, and the resulting precipitate was filtered off and dried, resulting in the formation of 3-bromo-1H-indazole intermediate **(Yield 70-72%).**

Step 2: Synthesis of 3-aryl indazole (211-212) [36]

In a solution of bromo compound (3-bromo-1H-indazole) (1 eq) and substituted boronic acid (1.2eq), in dioxane: water (3:1) caesium carbonate (2.5 eq) was added. The mixture was purged with nitrogen gas for 25-30 min. Further, tetrakis (5 mol%) was added, and the mixture was stirred at 125°C-130°C for 12 hr. The resulting mixture was then poured in ice cold water and extracted with ethyl acetate. The combined organic layers were washed with brine solution and dried using Na_2SO_4. The solvent was concentrated under vacuum, and the product was purified by flash chromatography with solvent system containing 50% ethyl acetate in hexane. The desired product was obtained with a yield of **50-60%**.

Step 3: Synthesis of N_1 alkylation of 3-Aryl indazole derivatives (213-222)

To a solution of 3-phenyl-1H indazole derivative (1 eq) in DMF was added potassium carbonate (4 eq) and the reaction mixture was stirred for 10 min at room temperature. Then 2-bromo-N-phenylacetamide derivative (1.3 eq), was added. The reaction mixture was stirred for 4–6 hr at room temperature, and ice-cold water was added. The formed precipitate was filtered off, dried, and recrystallized from 95% ethanol to furnish targeted derivatives at **70-80%** yield**.**

6.3. Biological investigation

In the present study, a panel of different human cancer cell lines were used for studying synthesized molecules for their effectiveness. The cell lines A-549 (lung cancer), MDA-MB-231 (triple negative breast cancer), MCF-7 (breast cancer), SiHa (cervical cancer)

along with normal mouse embryonic fibroblast cells (NIH/3T3) were obtained from National Centre for Cell Science (NCCS), Pune. These cell lines were chosen considering expression level of MCT1 and MCT4 or both for studying inhibitory effect of synthesized molecules. MDA-MB-231 cells predominantly expresses MCT4, SiHa and A-549 cells predominantly expresses MCT1 and MCT4, whereas MCF-7 expresses MCT1.

6.3.1 *In-vitro* Anticancer Activity

6.3.1.1 Investigation of initial set of compounds

6.3.1.1.1. Screening in MTT assay

A total of 68 target molecules were synthesized in initial phase, which includes coumarin, flavonoids, quinazoline, N-substituted benzylated indole and indazole cyanoacrylate derivatives. Series of all synthesized molecules were evaluated for their *invitro* cytotoxic activities against MCT1 and MCT4 overexpressing cell lines (SiHa, MDA-MB-231, MCF-7, and A-549) via MTT assay. Initially, two doses of each compound (10 µM and 25 µM) were evaluated. Reference inhibitor **IND CHC** was used as positive control and the vehicle DMSO was used as a negative control.

In the first set of series, we evaluated the coumarin compounds under normoxic conditions against MCT1 overexpressing SiHa cells using low glucose media. Here we found that compounds **10**, **11** and **12** showed good effect on cell viability (**figure 6**). This was comparable to the known MCT1 inhibitor **IND CHC**. We also carried out screening of the similar set of synthesized series against MDA-MB 231 cells, which are also known to express MCT4, and to a lesser extent MCT1. The results obtained in screening indicated that under normal media and incubation condition most of the compounds failed to show any substantial effect on cell viability (**figure 7**). Under normoxic condition using high

glucose media against SiHa cells, many compounds did not show effect on cell viability (**figure 8**).

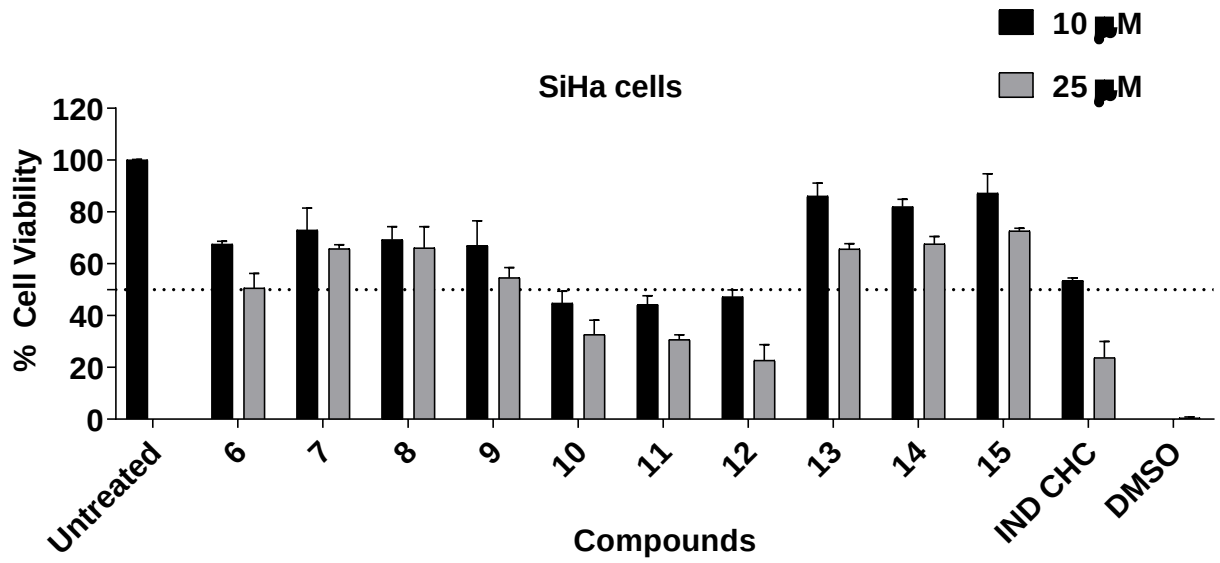

Figure 6: Screening of coumarin derivatives against SiHa cells in low glucose media in MTT assay

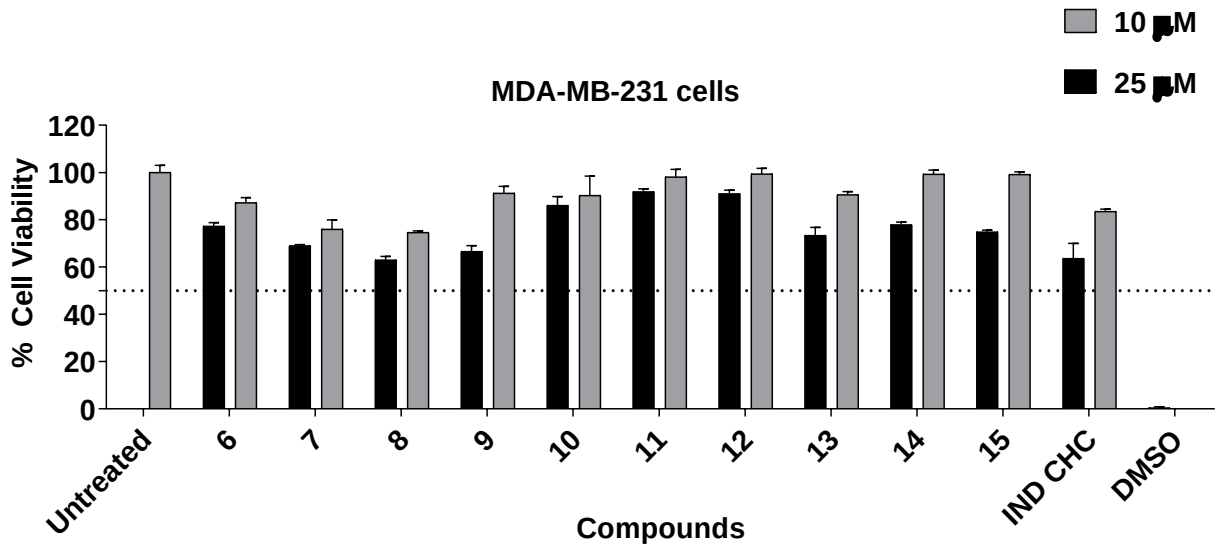

Figure 7: Screening of coumarin derivatives against MDA-MB-231 cells in low glucose media in MTT assay

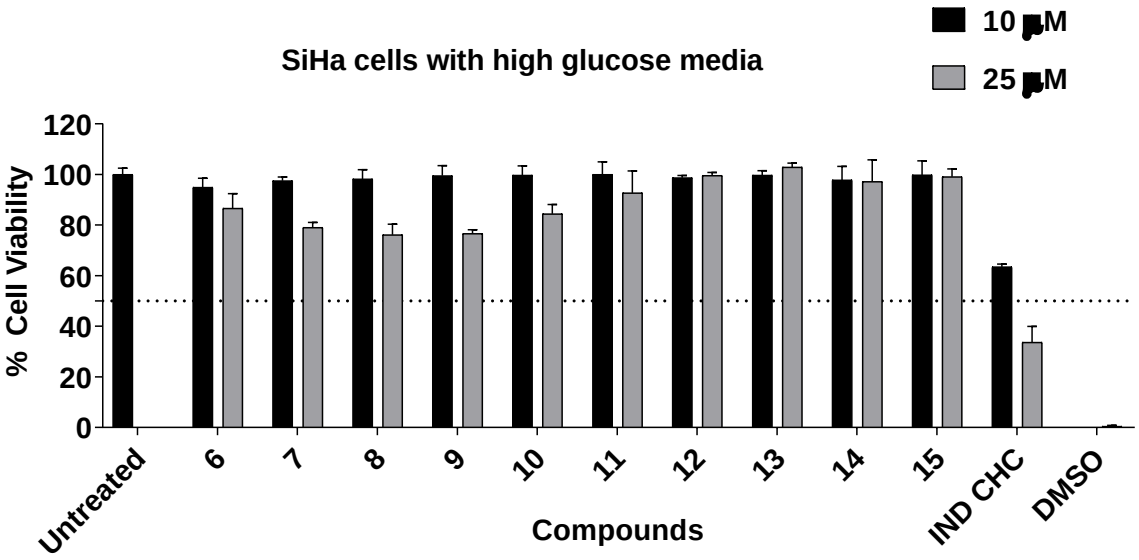

Figure 8: Screening of coumarin derivatives against SiHa cells in high glucose hypoxia media in MTT assay

In another set of series, we evaluate flavonoids and quinazoline based derivatives against MCT1 and MCT4 overexpressing cell lines (SiHa and MDA-MB-231). In the initial screening at 25 µM concentration, we found that none of the compound exhibited any MCT1 and MCT4 inhibition even at high concentration when compared with standard **IND CHC** (**figure 9-10).** Due to the lack of any MCT inhibition, we did not pursue the scaffold for any further development of MCT inhibitors.

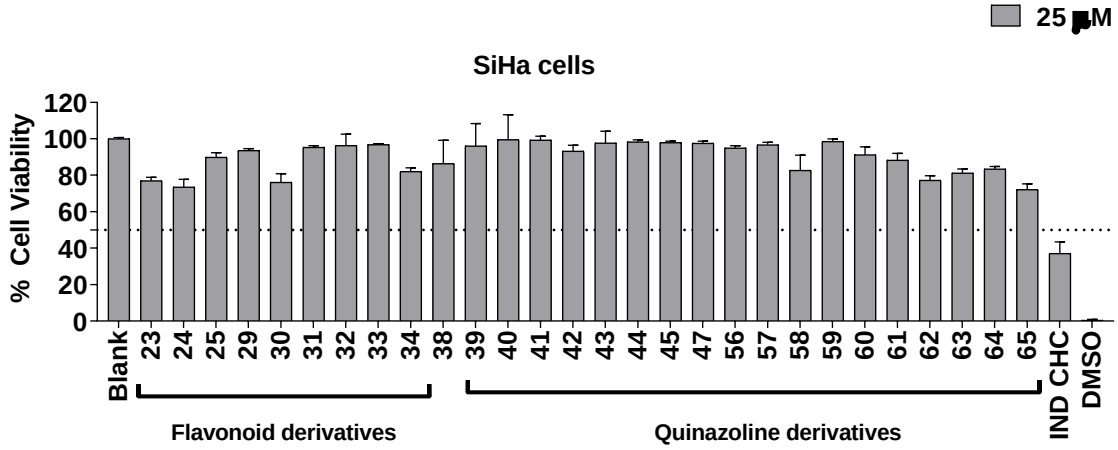

Figure 9: Screening of quinazoline and flavonoids derivatives against SiHa cells in MTT assay

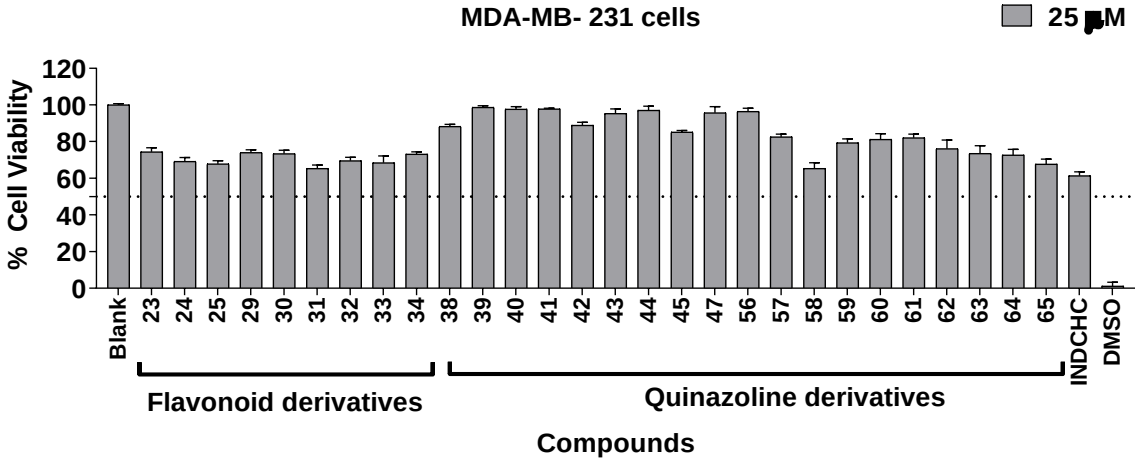

Figure 10: Screening of quinazoline and flavonoids derivatives against MDA-MB-231 cells in MTT assay

Since coumarin, flavonoids and quinazoline derivatives did not show any substantial effect against MCT1 and MCT4 expressing cells, we thought to preserve the cyanoacrylate moiety along with indole scaffold. Here we synthesized indole and indazole based derivatives linked with N-benzyl linker. After synthesizing, these compounds were evaluated for their MCT1 and MCT4 inhibition using predominantly MCT1 and MCT4 overexpressing A-549 and MDA-MB-231 cells respectively and **UK-5099** as a reference

standard (**figure 11-12**). The test result indicates that all the compounds are non-cytotoxic against A-549 and MDA-MB-231 cells even at 25 µM concentration.

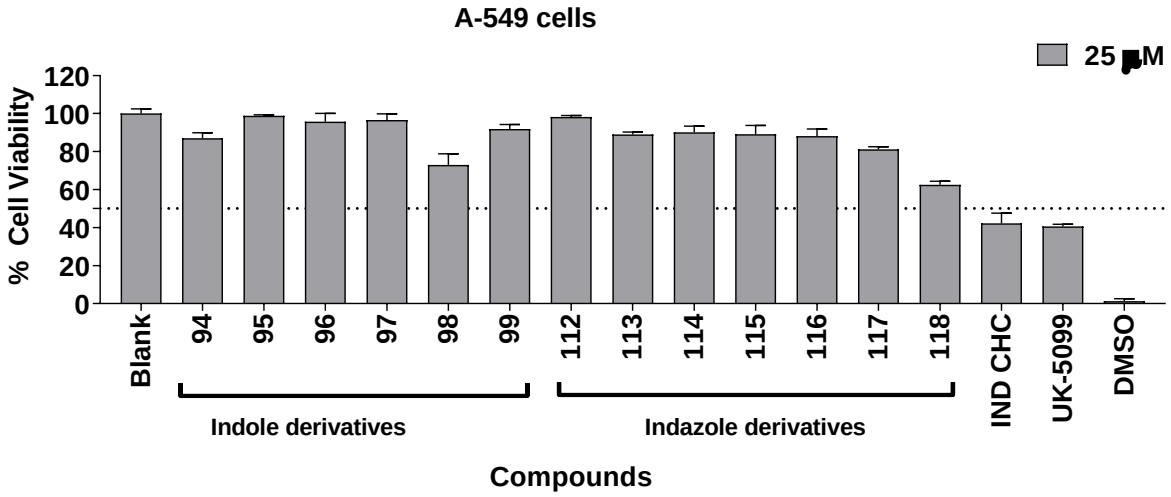

Figure 11: Screening of indole and indazole based derivatives against A-549 cells in MTT assay

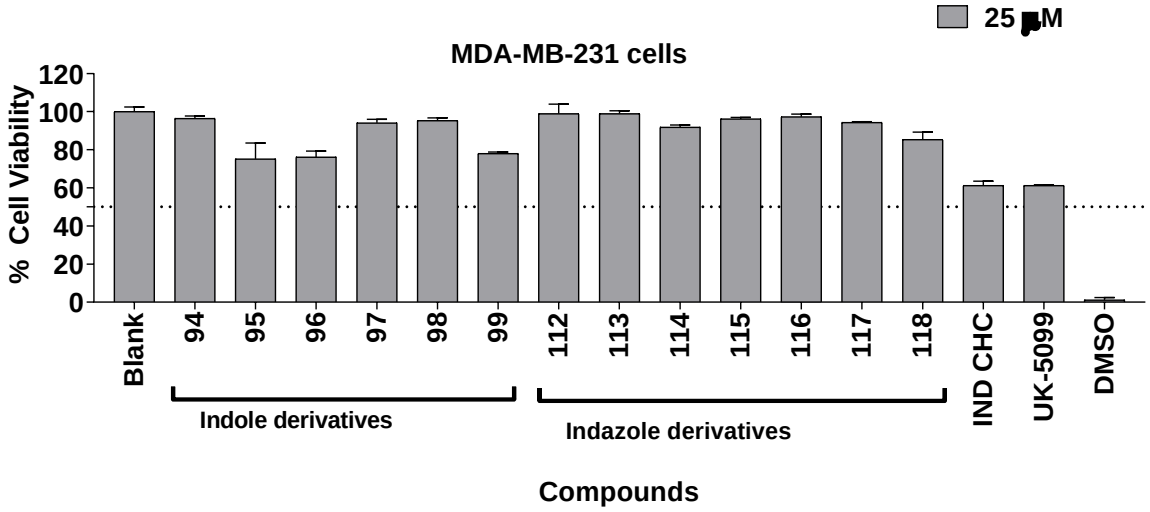

Figure 12: Screening of indole and indazole based derivatives against MDA-MB-231 cells in MTT assay

6.3.1.2. Investigation of indazole based compounds

6.3.1.2.1. Screening of indazole schiff based derivatives in MTT assay

Based on the results obtained from the previous study, indazole derivatives were functionalized by introducing imine moiety at 3rd position. Further all these derivatives were also evaluated against the MCT1 overexpressing (A-549, MCF-7) and MCT4 overexpressing (MDA-MB-231) cell line. Results obtained from initial screening indicate that none of the compound showed substantial activity against MCT1 and MCT4 even at 25 µM concentration when compared with standard MCT1 inhibitor (**figure 13-15)**. Further none of the compounds were found to be toxic against non-cancerous mouse embryonic fibroblast cell line (NIH/3T3) at final concentrations of 25 µM (**figure 16**). Based on this observation, selection of different target molecules was carried out. The final target scaffold selected for further biological evaluation includes indazole 3-carboxamide derivatives alkylated with N-phenyl acetamide and indole cyanoacrylate derivatives linked with N-phenyl acetamide based scaffold.

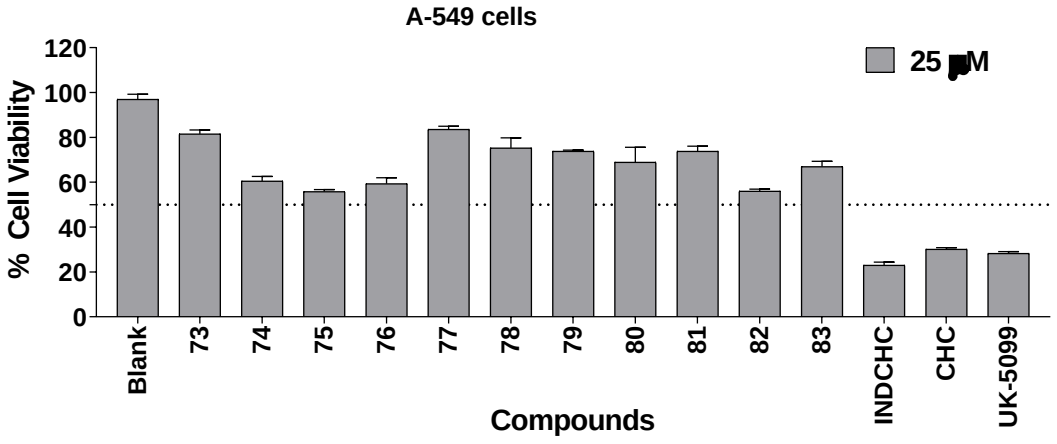

Figure 13: Screening of indole and indazole based derivatives against A-549 cell line in MTT assay

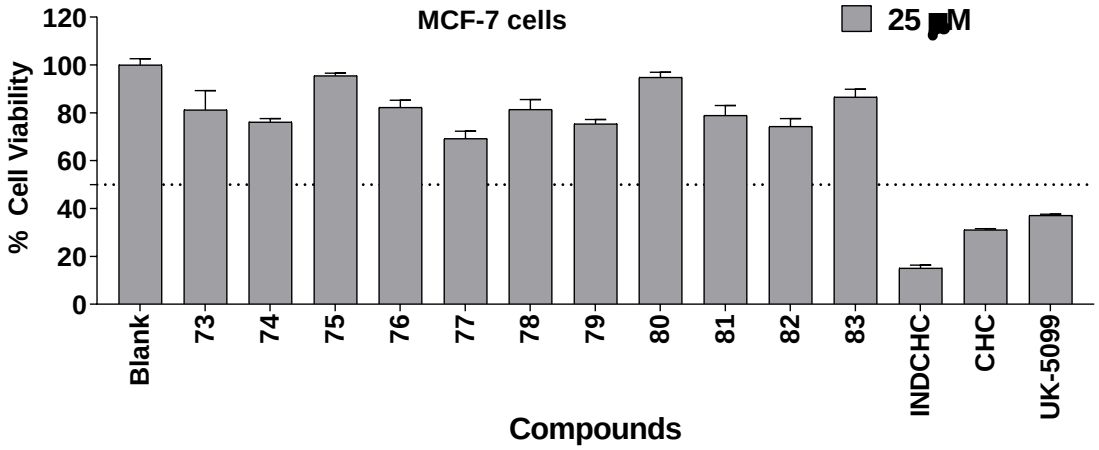

Figure 14: Screening of indole and indazole based derivatives against MCF-7 cells in MTT assay

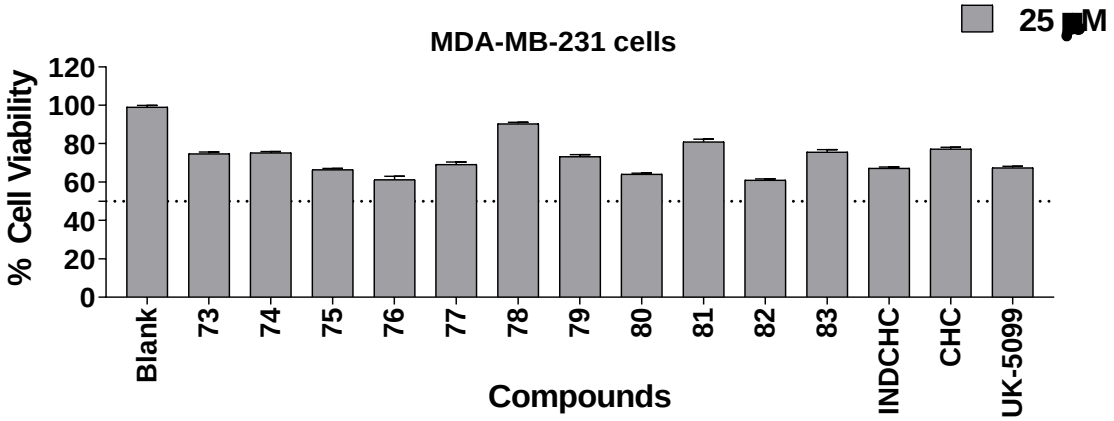

Figure 15: Screening of indole and indazole based derivatives against MDA-MB-231 cells in MTT assay

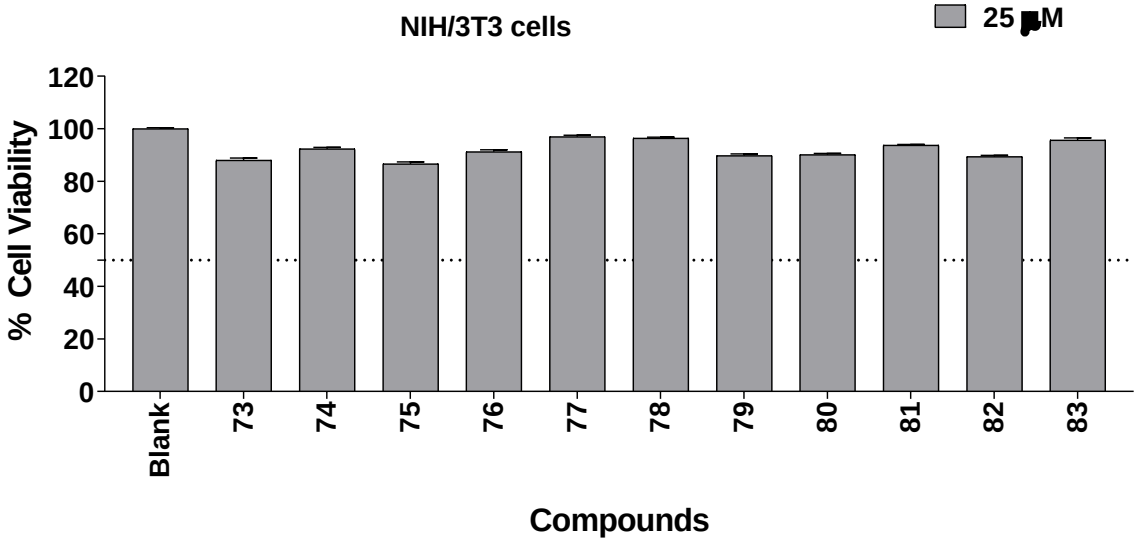

Figure 16: Screening of indole and indazole based derivatives against NIH/3T3 cells in MTT assay

6.3.1.2.2. Screening of indazole-3-carboxamide derivatives in MTT assay

A series of 36 indazole carboxamide derivatives were synthesized and evaluated for their cytotoxic activity against a panel of selected human cancer cell lines including A-549 MDA-MB-231, MCF-7, and NIH/3T3 using MTT assay. Initially, all the compounds were evaluated at 25 µM concentration by using **UK-5099** as reference standard. Among all synthesized compounds 16 derivatives (**138, 140, 148, 149, 157, 158, 159, 160, 161, 162, 165, 166, 167, 168, 171** and **172**) exhibited more than 50% inhibitory effects against A-549 cells (**Figure 17**), We found compound **167** showed highest potent inhibitory activity against A-549 cells. Similarly, screening against MDA-MB- 231 cells compounds **139, 146, 149, 152, 159, 160, 161, 162, 163, 165, 166, 168,** and **169** showed moderate to high inhibition (**Figure 18**). Among these compounds, compound **152** was the most potent. Similar derivatives were also screened against MCF-7 using **IND CHC**, **CHC** and **UK-5099** as a positive control. The result obtained from this screening suggested that 19

compounds (**137, 138, 139, 140, 141, 144, 145, 147, 153, 154, 155, 156, 157, 158, 159, 160, 161, 168** and **169**) have good inhibitory activity against MCF-7 cells **(Figure 19)**. Among these, **137** turned out to be the most cytotoxic towards MCF-7 cells. Screening against NIH/3T3 cells suggested that these compounds did not have any cytotoxic effect against non-cancerous fibroblast cells (**Figure 20**). Molecules displaying >50% inhibition of cell viability at 25 µM concentrations in MTT assay screening were further selected for GI_{50} determination. The GI_{50} values of these compounds are summarized in **Table 1.** The predicted structure activity relationship is illustrated in **Figure 21.**

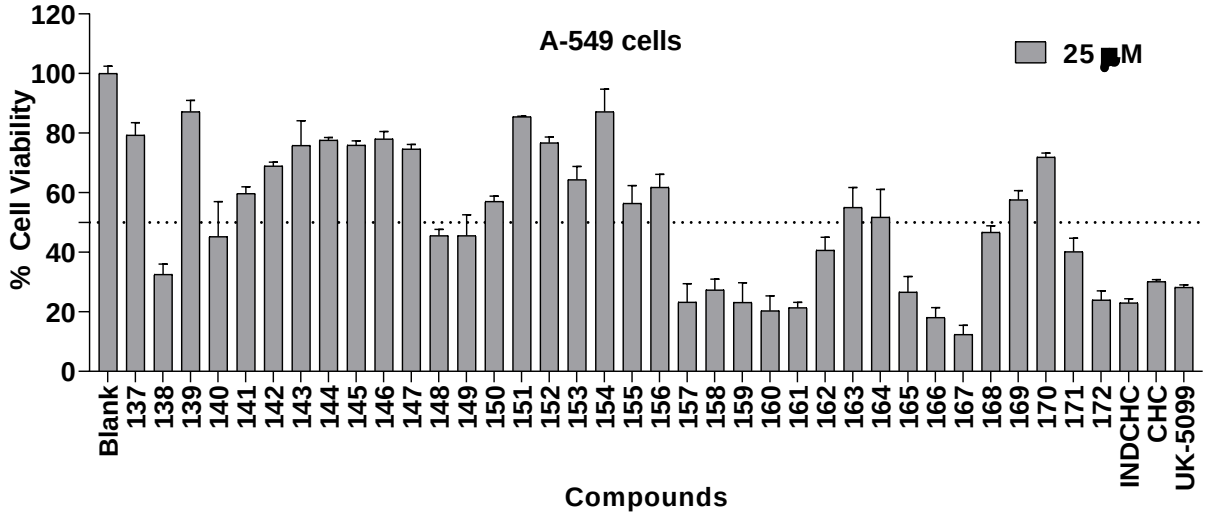

Figure 17: Screening of indazole-3-carboxamide derivatives against A-549 cells in MTT assay

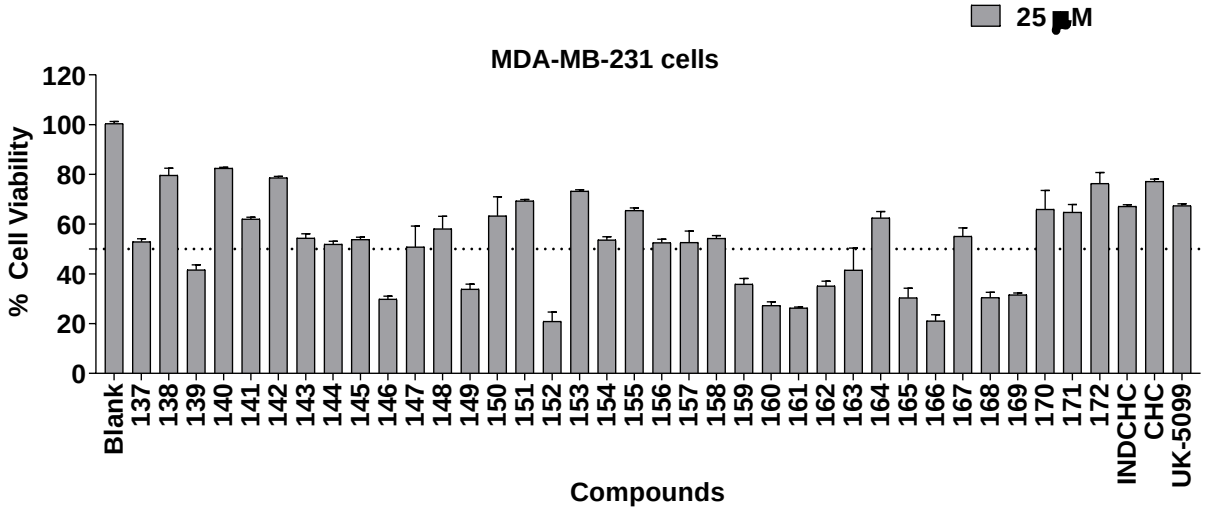

Figure 18: Screening of indazole-3-carboxamide derivative against MDA-MB-231 cells in MTT assay

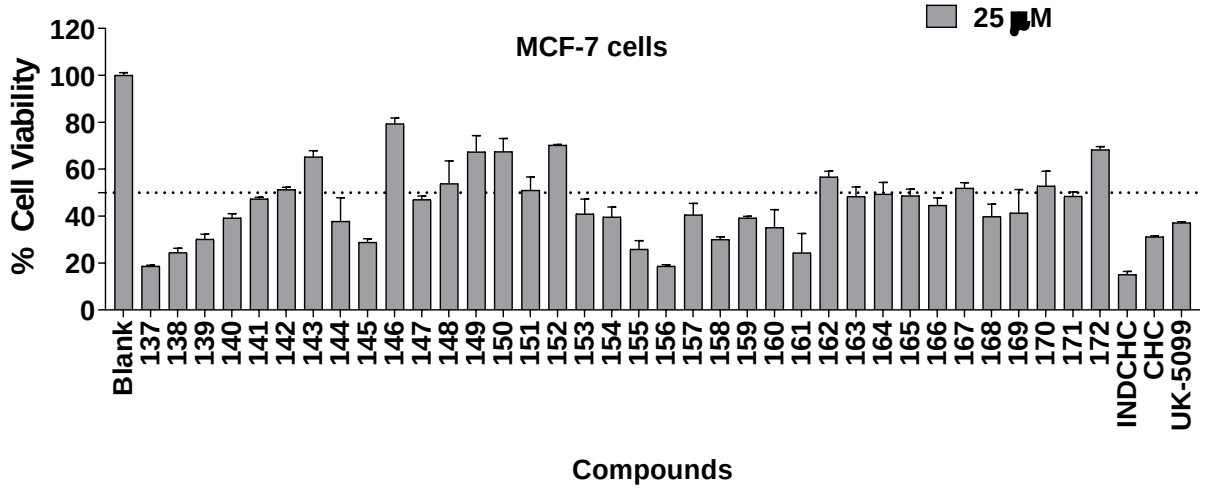

Figure 19: Screening of indazole-3-carboxamide derivative against MCF-7 cells in MTT assay

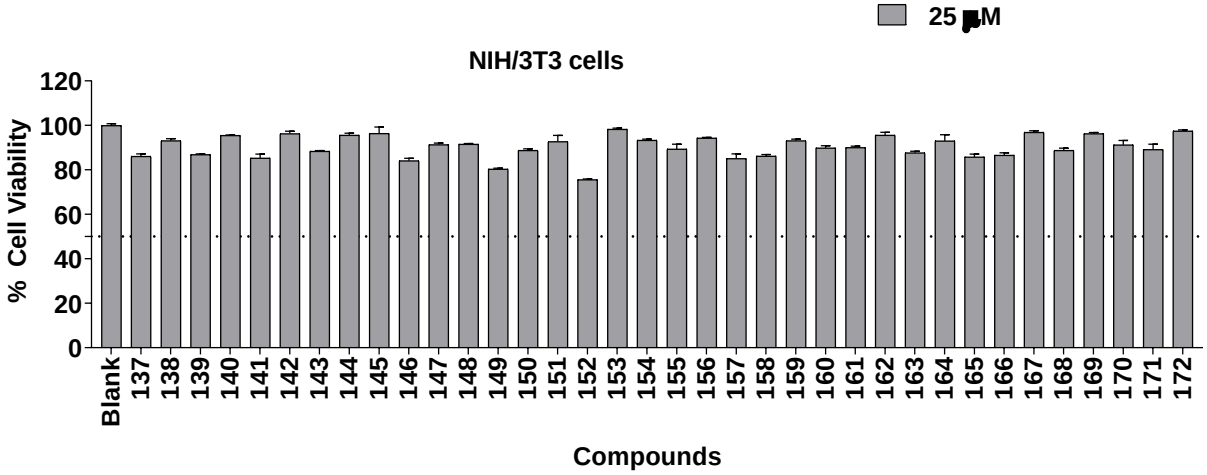

Figure 20: Screening of indazole-3-carboxamide derivative against NIH/3T3 cells in MTT assay

Table 1: *In-vitro* anticancer activity of indazole derivatives

Compound code	GI_{50} (µM ± SD)		
	MDA-MB-231	A-549	MCF-7
137	ND	ND	2.34 ± 0.036
138	ND	22.9 ± 0.014	36.98 ± 0.019
139	19.97 ± 0.022	ND	3.21 ± 0.033
140	ND	38.04 ± 0.020	ND
144	ND	ND	13.35 ± 0.023
145	ND	ND	4.93 ± 0.038
146	25.88 ± 0.020	ND	ND
148	ND	35.46 ± 0.015	ND
150	27.93 ± 0.018	37.98 ± 0.013	ND
152	17.29 ± 0.030	ND	ND
153	ND	ND	17.61 ± 0.029
154	ND	ND	20.06 ± 0.029
155	ND	ND	29.21 ± 0.02
156	ND	ND	24.04 ± 0.039
157	ND	32.77 ± 0.022	29.72 ± 0.029

158	ND	21.51 ± 0.025	38.8 ± 0.022
159	26.4 ± 0.085	19.77 ± 0.028	14.67 ± 0.020
160	20.07 ± 0.029	15.71 ±0.044	27.78 ± 0.012
161	18.97 ± 0.028	19.17 ± 0.027	30.19 ±0.032
162	21.68 ± 0.036	27.27 ± 0.019	ND
163	25.17 ± 0.035	ND	ND
164	ND	37.14 ± 0.016	ND
165	26.68 ± 0.025	30.35 ± 0.0128	25.55 ± 0.027
166	18.31 ± 0.027	26.50 ±0.020	ND
167	ND	14.3 ± 0.020	ND
168	31.34 ± 0.031	28.62 ± 0.010	10.82 ± 0.025
169	31.4 ± 0.022	ND	20.7 ± 0.029
171	ND	31.24 ± 0.010	ND
172	ND	20.89 ± 0.016	ND
UK-5099	inactive	10.25 ± 0.025	14.65 ± 0.042

Where, ND = Not determined, GI_{50} = Required concentration of compounds for inhibition of cell growth by 50%, **UK-5099** = Standard inhibitor.

6.2.1.2.3. Structure activity relationship of indazole-3-carboxamide derivatives

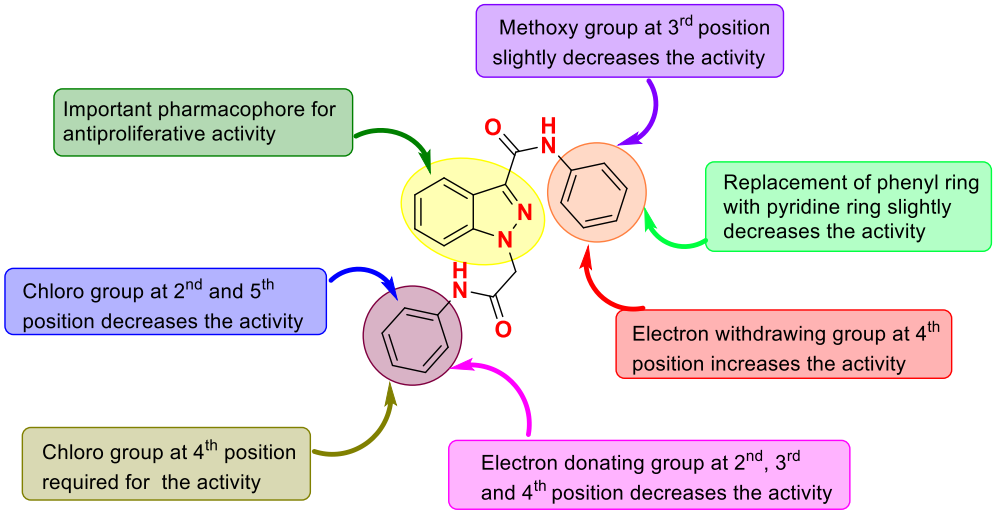
Methoxy group at 3rd position slightly decreases the activity
Important pharmacophore for antiproliferative activity
Replacement of phenyl ring with pyridine ring slightly decreases the activity
Chloro group at 2nd and 5th position decreases the activity
Electron withdrawing group at 4th position increases the activity
Chloro group at 4th position required for the activity
Electron donating group at 2nd, 3rd and 4th position decreases the activity

Figure 21: Structure-activity relationship of indazole-3-carboxamide derivatives for their antiproliferative activity

6.3.1.3 Investigation of indole-based compounds

6.3.1.3.1 Screening of indole-3- cyanoacrylate derivatives in MTT assay

After investigating indazole based molecules, we synthesized 16 indole-based derivatives by preserving cyanoacrylate moiety at the 3rd position of the indole scaffold (as in **UK-5099**). A N-phenylacetamide linker was introduced at the N1 position of indole. These molecules were evaluated against MCT1 (A-549, MCF-7) and MCT4 (MDA-MB-231) overexpressing cells. Results obtained from screening at 25 µM concentration indicate that all compound exhibited >50% cell growth inhibition in all tested cells. Among tested series, compounds **178**, **181**, **186, 188, 189,** and **190** showed the most promising antiproliferative activity against A-549 cells when compared with reference standard (**Figure 22**). A similar experiment was also performed on MDA-MB-231 cells. Screening reveals that all the compounds exhibited >50% inhibition at 25 µM concentration, among which compounds **179, 184** and **190** showed promising inhibitory activity towards MDA-MB-231 cells (**Figure 23**). Further these molecules were screened against MCF-7 cells. The results obtained from this screening suggested all synthesized compounds (**176-191**) showed good inhibitory activity against MCF-7 cells **(Figure 24)**, among these **178, 190** and **191,** turned out to be the most effective against MCF-7 cells. Cellular toxicity of indole cyanoacetate derivatives was also evaluated against normal mouse embryonic fibroblast cells (NIH/3T3). Results obtained from this screening suggested that none of the compounds had cytotoxic effect against non-cancer cells (**Figure 25**). The GI_{50} values of these compounds are summarized in **Table 2.** The predicted structure activity relationship is illustrated in **Figure 26.**

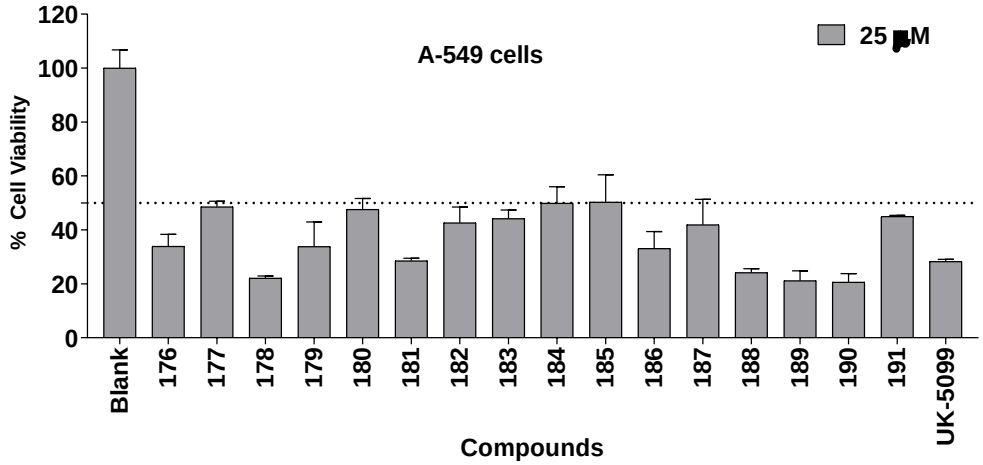

Figure 22: Screening of indole-3- cyanoacrylate derivatives against A-549 cells in MTT assay

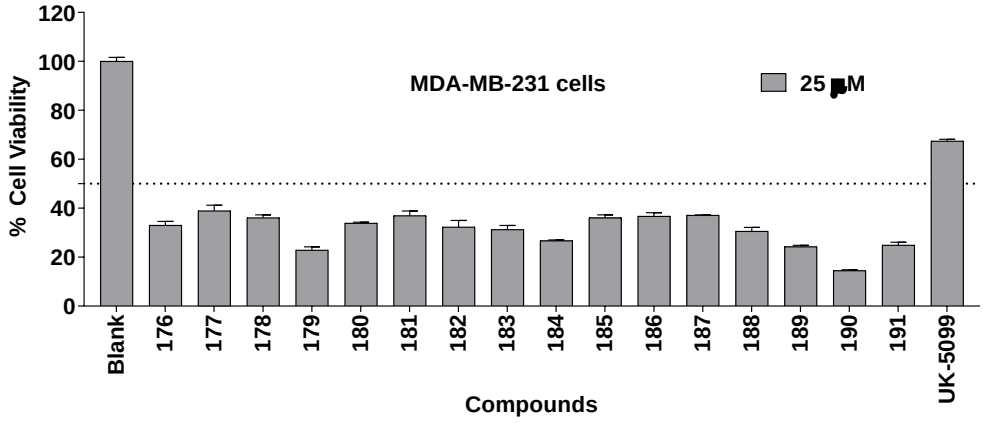

Figure 23: Screening of indole-3- cyanoacrylate derivatives against MDA-MB-231 cells in MTT assay

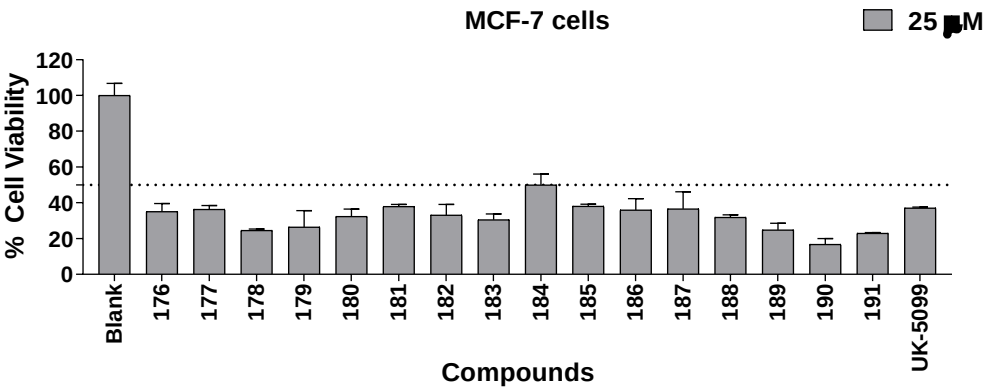

Figure 24: Screening of indole-3- cyanoacrylate derivatives against MCF-7 cells in MTT assay

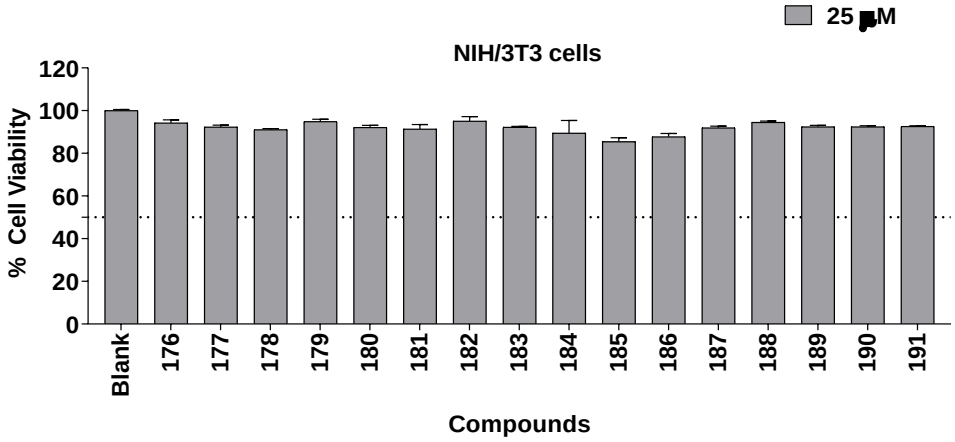

Figure 25: Screening of indole-3- cyanoacrylate derivatives against NIH/3T3 cells in MTT assay

Table 2: *In-vitro* anticancer activity of indole cyanoacrylate derivatives

Compound code	GI_{50} (µM ± SD)		
	A-549	MDA-MB-231	MCF-7
176	29.23 ± 0.23	26.06 ± 0.3	15.39 ± 0.33
177	19.2 ± 0.2	25.73 ± 0.32	9.99 ± 0.46
178	13.97 ± 0.48	27.27 ± 0.48	13.92 ± 0.1
179	21.53 ± 0.35	25.2 ± 0.12	15.4 ± 0.47
180	17.1 ± 0.44	24.03 ± 0.15	4.32 ± 0.14
181	26 ± 0.25	31.77 ± 0.82	19.1 ± 0.46
182	28.3 ± 0.1	25.3 ± 0.45	15.27 ± 0.01
183	20.9 ± 0.42	24.97 ± 0.35	10.7 ± 0.38
184	19.97 ± 0.64	23.4 ± 0.17	15.08 ± 0.39
185	26.87 ± 0.33	21.43 ± 0.09	15.46 ± 1.34

186	25.47 ± 0.47	27.37 ± 0.45	14.69 ± 0.21
187	24.7 ± 0.47	18.77 ± 0.66	17.33 ± 0.57
188	21.97 ± 0.55	11.73 ± 0.03	15.14 ± 0.31
189	18.83 ± 0.23	17.17 ± 0.24	3.13 ± 0.23
190	19.33 ± 0.29	9.31 ± 0.21	9.12 ± 0.22
191	19.23 ± 0.41	21.4 ± 0.42	11.06 ± 0.15
UK-5099	10.25 ± 0.025	>100 μM	14.65 ± 0.042

6.3.1.3.2. Structure activity relationship of indole-3- cyanoacrylate compounds

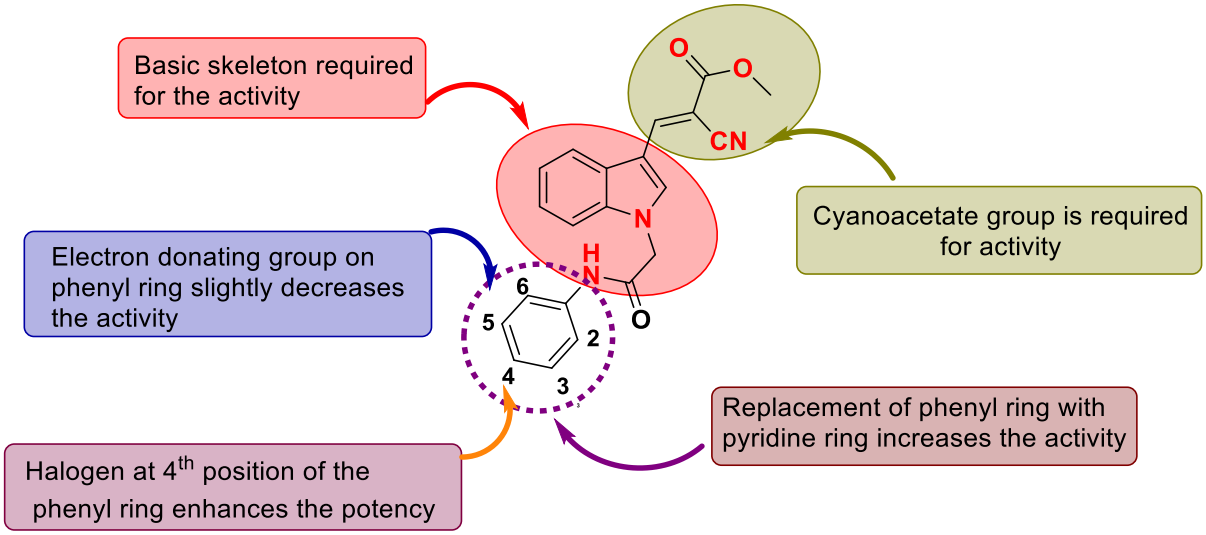

Figure 26: Structure activity relationship of indole-3-cyanoacrylate derivatives for their antiproliferative activity

6.3.1.4. Investigation of indazole based compounds linked with N-phenyl propanamide derivatives

6.3.1.4.1 Screening of indazole based compounds linked with N-phenyl propanamide derivatives

Inspired by the results obtained from previous study, we functionalized the indazole moiety by retaining the carboxamide moiety at 3rd position of the indazole and replacing N1 position with N-phenylpropanamide linker. Here we synthesized 13 derivatives and screened against MCT1 overexpressing (A-549 and MCF-7) and MCT4 overexpressing

(MDA-MB-231) cells at 25 µM concentration by using **UK-5099**, **CHC** and **IND CHC** as positive control. Results obtained from screening revealed that compound **209** showed most potent inhibitory effect against A-549 cells (**figure 27**). Whereas it was observed that compound **207** exhibited excellent antiproliferative activity against the MCT-1 overexpressing MCF-7 cells (**figure 28**). A similar set of experiment carried out against MCT-4 overexpressing MDA-MB-231 cells, showed that compound **206** has a good inhibitory activity (**figure 29**). Further, cytotoxicity of synthesized compounds was also investigated against normal mouse embryonic fibroblast cells (NIH/3T3) to check whether the synthesized compound shows effect on growth of non-cancer normal cells. Results obtained indicated that none of the synthesized compounds affected growth of non-cancer cells. This indicated the selective targeting of compounds towards cancer cells (**figure 30**). The GI_{50} values of these compounds are summarized in **Table 3.** The predicted structure activity relationship is illustrated in **Figure 31.**

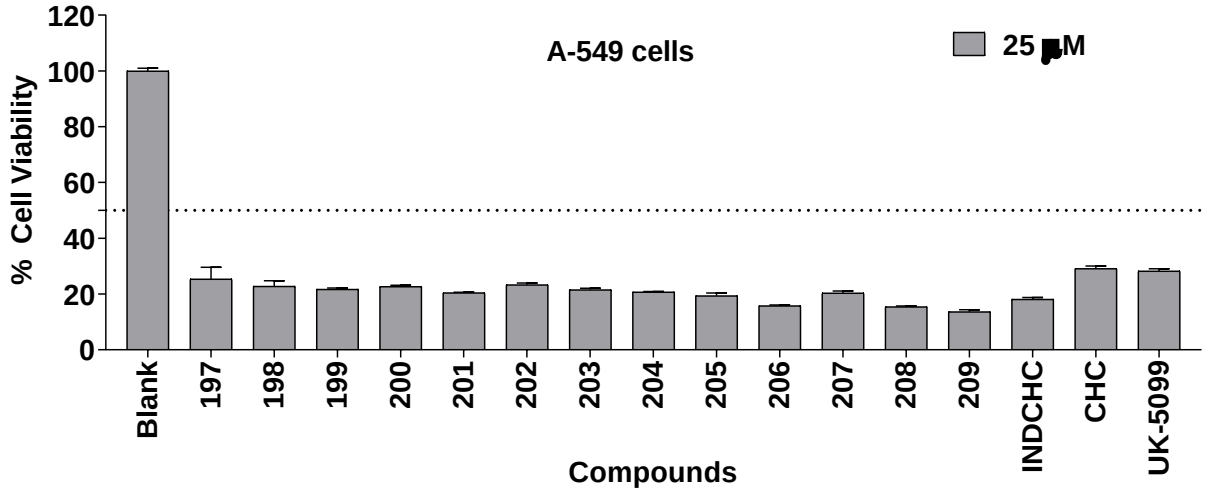

Figure 27: Screening of indazole based compounds linked with N-phenylpropanamide derivatives against A-549 cells in MTT assay

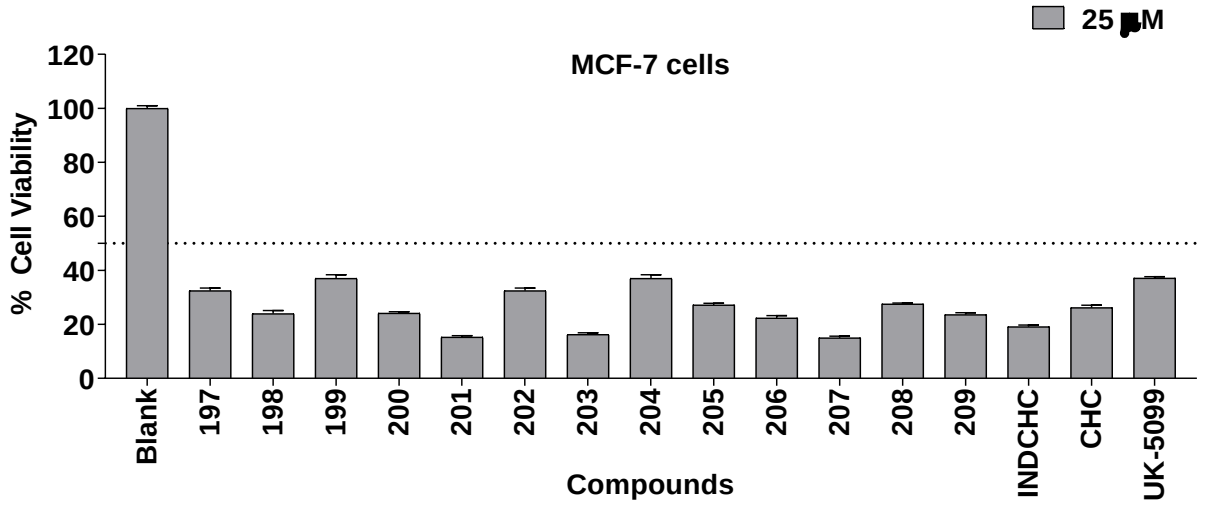

Figure 28: Screening of indazole based compounds linked with N-phenylpropanamide derivatives against MCF-7 cells in MTT assay

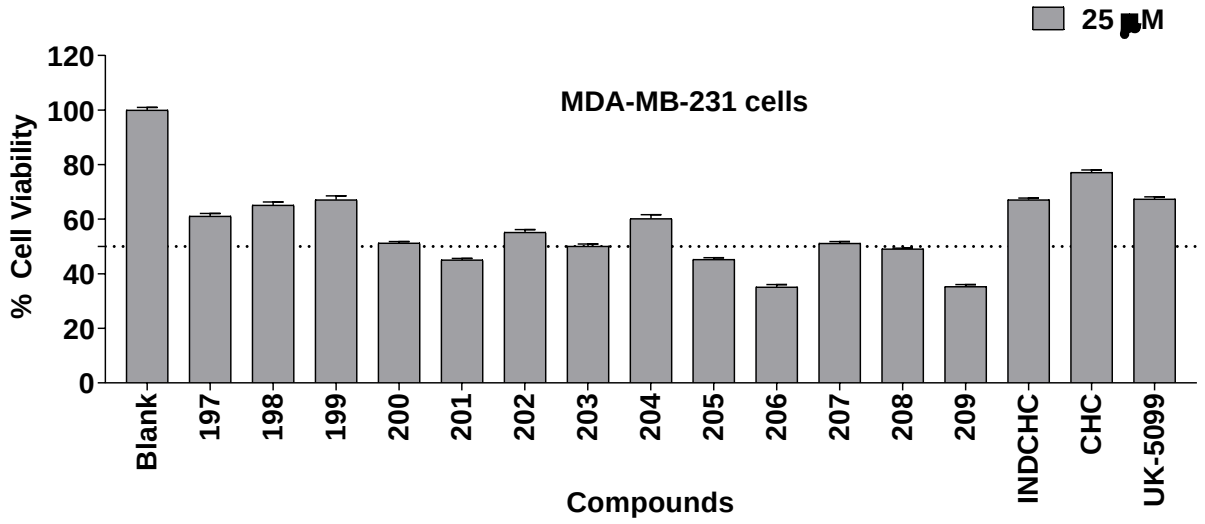

Figure 29: Screening of indazole based compounds linked with N-phenylpropanamide derivatives against MDA-MB-231 cells in MTT assay

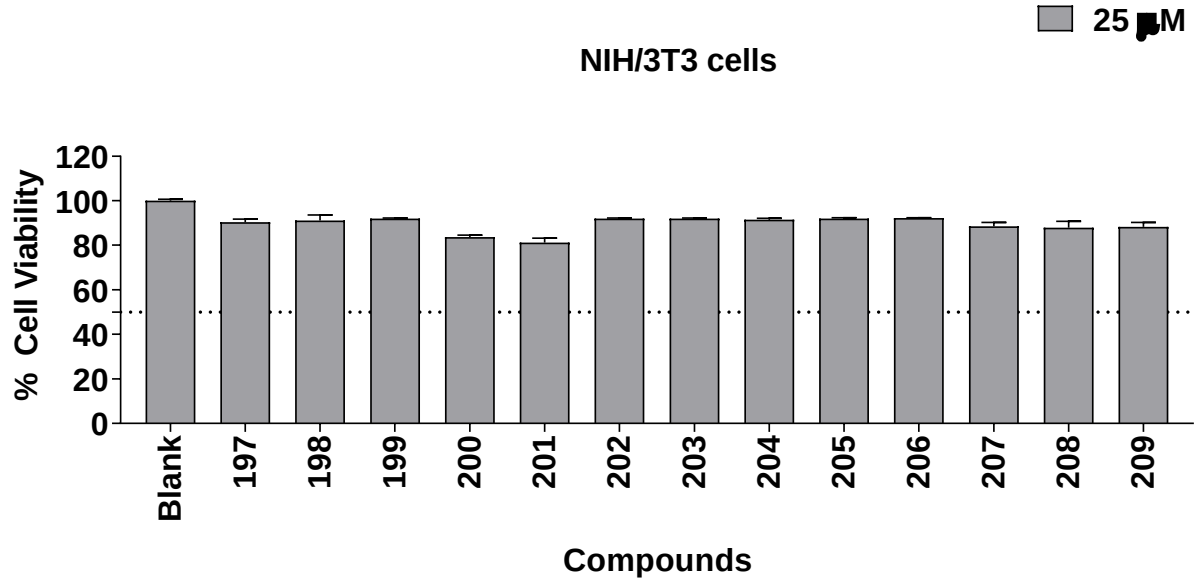

Figure 30: Screening of indazole based compounds linked with N-phenylpropanamide derivatives against NIH/3T3 cells in MTT assay

Table 3: In-vitro antiproliferative activity of indazole based compounds linked with N-phenylpropanamide derivatives

	GI50 (µM ± SD)

Compound code	A-549	MCF-7	MDA-MB-231
197	7.87 ± 0.06	11.52 ± 0.25	nt
198	17.42 ± 0.11	14.17 ± 0.17	nt
199	15.61 ± 0.48	13.86 ± 0.34	nt
200	15.83 ± 0.24	7.88 ± 0.15	nt
201	12.73 ± 0.2	11.82 ± 0.12	nt
202	7.84 ± 0.25	12.85 ± 0.13	nt
203	15.01 ± 0.48	12.49 ± 0.24	14.99 ± 0.45
204	12.49 ± 0.25	15.96 ± 0.35	nt
205	14.98 ± 0.21	12.1 ± 0.09	11.58 ± 0.04
206	12.05 ± 0.33	12.23 ± 0.16	10.31 ±0.28
207	11.67 ± 0.44	10.37 ± 0.11	nt
208	11.96 ± 0.23	12.04 ± 0.22	nt
209	10.99 ± 0.25	12.47±0.2	18.36 ± 0.37
UK-5099	10.25 ± 0.025	14.65 ± 0.042	>100

6.2.1.4.2. Structure activity relationship of indazole based compounds linked with N-phenylpropanamide derivatives

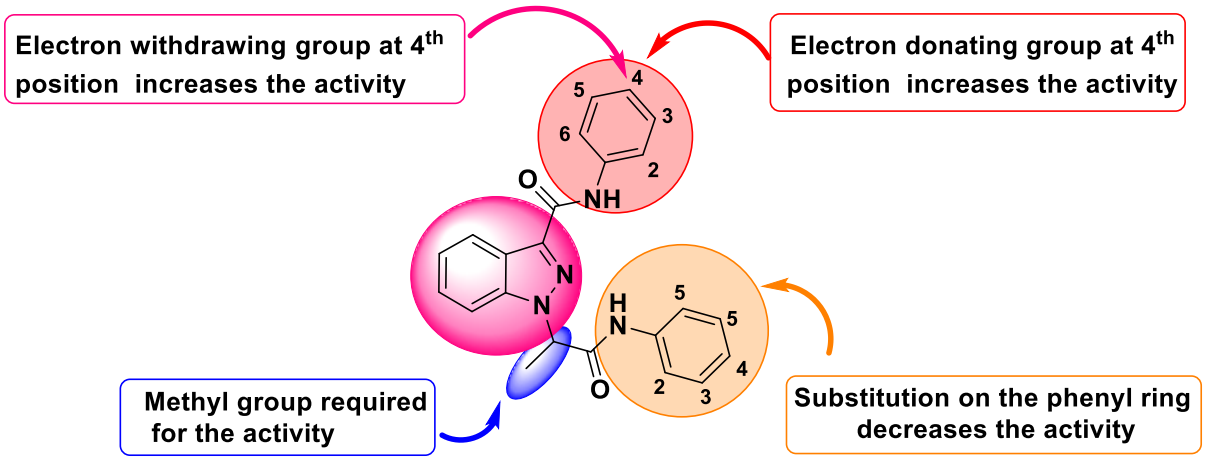

Figure 31: Structure activity relationship of indazole based compounds linked with N-phenylpropanamide derivatives for their antiproliferative activity

6.3.1.5. Investigation of 3-phenylindazole based compounds linked with N-phenylacetamide derivatives

6.3.1.5.1. Screening of 3-phenyl indazole based compounds linked with N-phenylacetamide derivatives

In the last set of indazole based molecules, we carried out modification in indazole scaffold by replacing the 3-carboxamide moiety with 3-aryl group, while keeping the N-phenylacetamide linker same. These molecules were also examined for their ability to inhibit growth of A-549, MCF-7, MDA-MB-231 cells by MTT assay. We also examined the cytotoxicity of synthesized molecules against non-cancer mouse embryonic fibroblast NIH/3T3 cells to check the selectivity. The screening results indicated that all synthesized compounds have moderate to good antiproliferative activity against all carcinoma cells. Among the series of synthesized compounds, compounds **218** and **221** displayed better inhibitory activity against A-549 and MCF-7 cells respectively. It was observed that compound **221** also possesses the ability to inhibit the MDA-MB-231 cells. Graphical representation of the biological screening is shown in **figure 32-34.** None of the synthesized compounds exhibited cytotoxicity against non-cancer NIH/3T3 cells **(figure 35).** The GI_{50} values of these compounds are summarized in **Table 4.** The predicted structure activity relationship is illustrated in **Figure 36.**

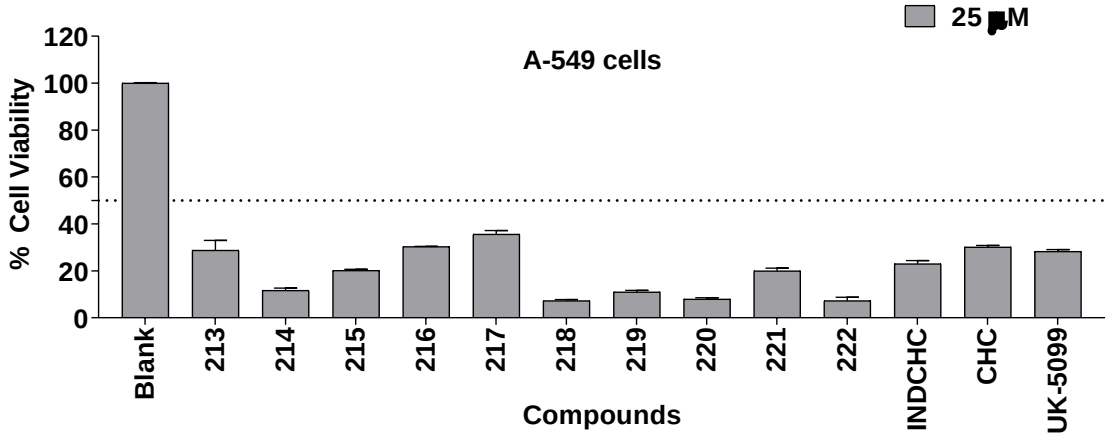

Figure 32: Screening of 3-phenylindazole based compounds linked with N-phenylacetamide derivatives against A-549 cells in MTT assay

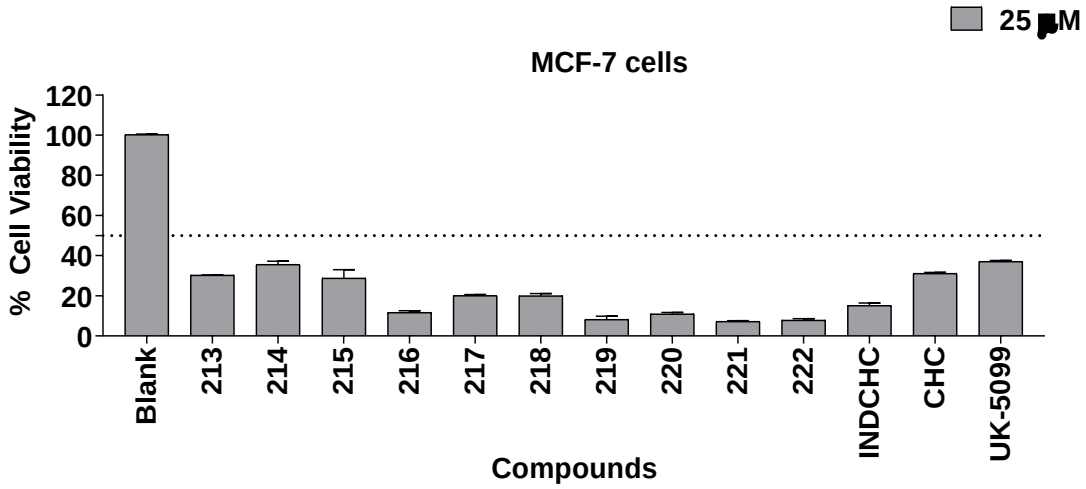

Figure 33: Screening of 3-phenylindazole based compounds linked with N-phenylacetamide derivatives against MCF-7 cells in MTT assay

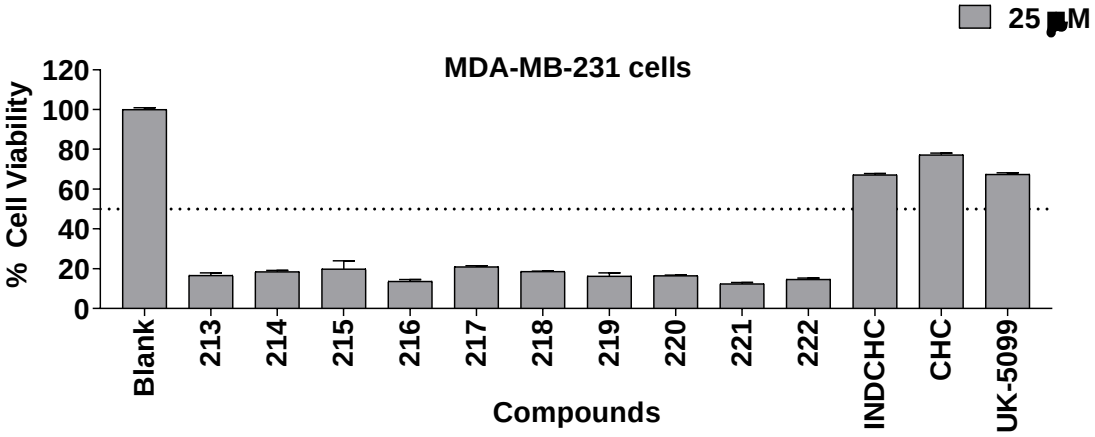

Figure 34: Screening of 3-phenylindazole based compounds linked with N-phenylacetamide derivatives against MDA-MB-231 cells in MTT assay

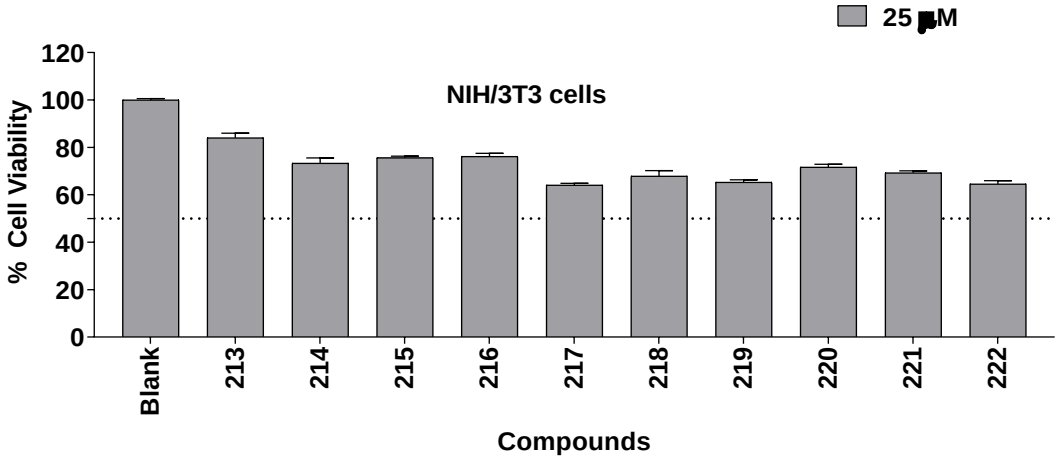

Figure 7: Screening of 3-phenylindazole based compounds linked with N-phenylacetamide derivatives against NIH/3T3 cells in MTT assay

Table 4: *In-vitro* antiproliferative activity of 3-phenylindazole based compounds linked with N-phenylacetamide derivatives

Compound code	GI_{50} (µM ± SD)		
	A-549	MCF-7	MDA-MB-231
213	12.02 ± 0.21	11.39 ± 0.49	10.13 ± 0.31
214	16.51 ± 0.57	11.11 ± 0.13	15.02 ± 1.24
215	11.93 ± 0.49	9.73 ± 0.08	9.43 ± 0.25
216	7.89 ± 0.18	8.87 ± 0.12	6.66 ± 0.5
217	9.7 ± 0.08	10.75 ± 0.19	12.17 ± 0.62

218	9.58 ± 0.3	10 ± 0.22	8.62 ± 0.12
219	12.22 ± 0.24	11.44 ± 0.19	9.61 ± 0.96
220	8.95 ± 0.24	9.27 ± 0.24	6.94 ± 0.22
221	9.79 ± 0.11	9.44 ± 0.24	11.7 ± 1.63
222	8.14 ± 0.73	8.46 ± 0.27	14.29 ± 1.41
UK-5099	10.25 ± 0.025	14.65 ± 0.042	>100

6.2.1.5.2. Structure activity relationship of 3-phenylindazole based compounds linked with N-phenylacetamide derivatives

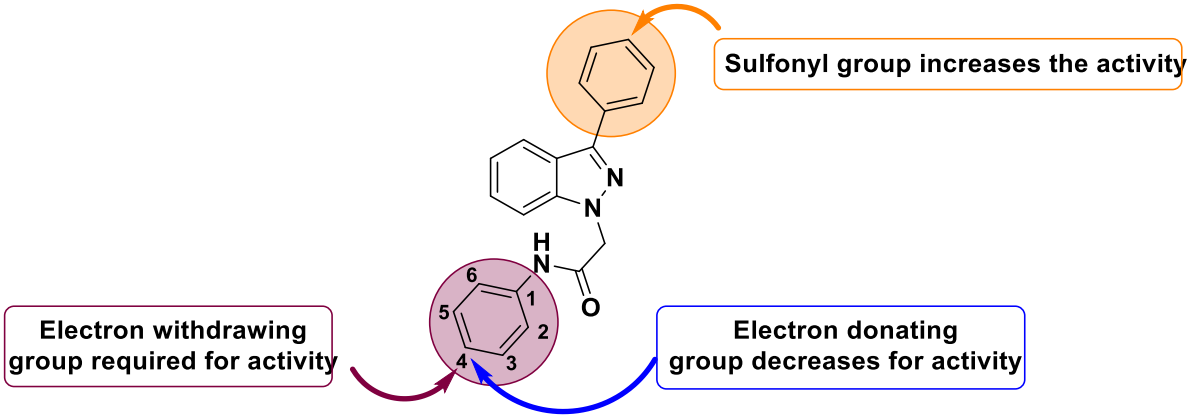

Figure 36: Structure activity relationship of 3-phenylindazole based compounds linked with N-phenylacetamide derivatives for their antiproliferative activity

6.4. Functional assay

6.4.1. 3-Bromopyruvate assay for studying MCT1 inhibition

6.4.1.1. Indazole-3-carboxamide derivatives

The inhibitory activity of indazole and indole-based derivatives against MCT1 was determined by using 3-bromopyruvate (3-BP) functional assay. In the first phase of study indazole-3-carboxamide derivatives were screened for their MCT1 inhibition against MCT1 overexpressing A-549 cells at 5 µM concentration. Here, MCT1-expressing A-549 cells, were exposed to the MCT1 substrate 3-BP, which influxed by MCT1 intracellularly.

3-BP is a cytotoxic molecule which decreases cell viability. Inhibition of MCT1 results in reduced intracellular accumulation 3-BP levels and, thus, reduced inhibition of cell compared to no inhibition of MCT1. The half-maximal growth inhibition (GI_{50}) value of 3-BP was found to be 25.0 ± 0.4 µM. As 50 µM 3-BP inhibited A-549 cell growth by ≥90% (GI_{90} = 49.8 ± 0.6 µM), this concentration was used to assess the inhibitory activity of indazole derivatives. Synthesized compounds were screened at 5 µM concentration. Results obtained from the screening suggested that among all tested compounds only 15 compounds (**148, 149, 157, 158, 159, 160, 161, 162, 164, 165, 166, 167, 168, 171,** and **172)** showed the ability to reduce the toxicity of 3-BP and enhanced the cell viability. Screening of test compounds was carried out in comparison with reference MCT1 inhibitor such as **UK-5099**. MCT1 inhibitory activity of indazole derivatives is shown in **Figure 37.** Molecules displaying > 50% of cell viability at 5 µM concentrations were further taken up for IC50 determination by using different concentrations (100 nm to 5 µM). IC50 value of the potent compounds are given in **table 5**.

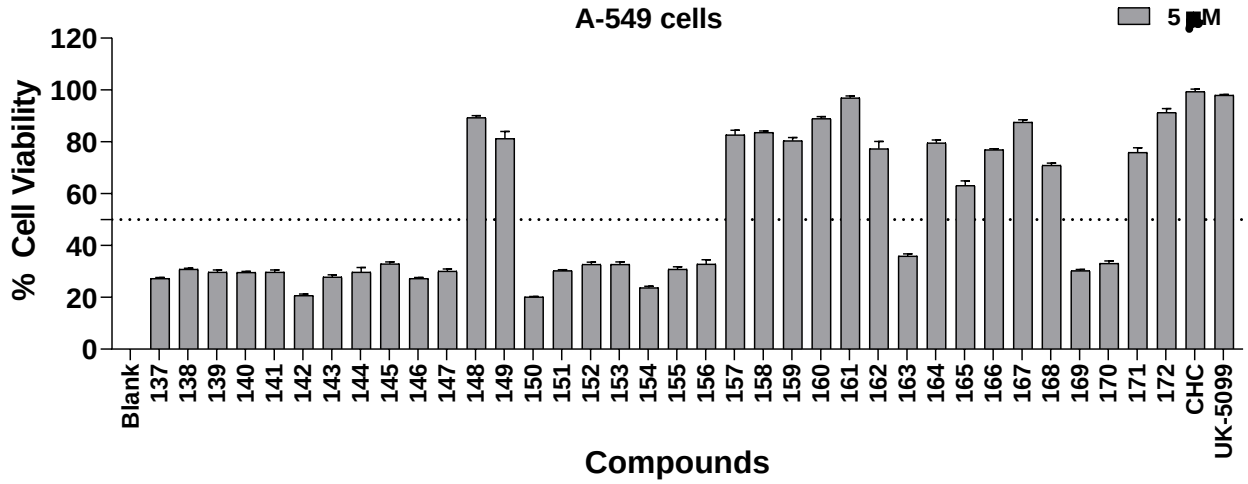

Figure 37*:* MCT1 inhibitory activity of indazole-3-carboxamide derivatives against A-549 cells in 3-BP assay

Table 5: MCT1 inhibitory activity of indazole-3-carboxamide derivatives against A-549 cells

Compound code	A-549 (MCT1 inhibition) (IC_{50} ± SD)
148	2.24 ± 0.02 µM
149	3.47 ± 0.06 µM
157	3.87 ± 0.06 µM
158	4.13 ± 0.47 µM
159	3.12 ± 0.08 µM
160	3.78 ± 0.06 µM
161	1.02 ± 0.03 µM
162	3.15 ± 0.10 µM
164	1.88 ± 0.05 µM
165	4.02 ± 0.06 µM
166	3.75 ± 0.09 µM
167	1.65 ± 0.05 µM
168	3.24± 0.05 µM
171	1.67 ± 0.04 µM
172	3.87 ± 0.07 µM
UK-5099	0.17 ± 0.03 µM

6.4.1.2 Indole 3-cyanoacrylate derivatives

Another set of 16, 3-cyanoacrylate derivatives was also evaluated for their MCT1 inhibition against MCT1 overexpressing A-459 cells. The results obtained from the study suggested that all indole derivatives possess high inhibitory potential in sub-micromolar concentration ranges. The lead compound **176** with a phenyl substitution at the amide linker possessed an IC_{50} value of 314 nM. Only compound **188** with a 4-flourine substitution showed weaker MCT1 inhibition (IC_{50} = 793 nM). Substitution at 4^{th} position on the phenyl ring of N-acetamido linker (**177, 178, 183, 184** and **185**) and para-halogen substitutions (**177** and **183**) led to a very strong increase in the inhibitory potential. Compound **184** with its 4-methoxy substitution showed the highest MCT1 transport inhibition with an IC_{50} value of 81.0 nM, which is better than reference MCT1 inhibitor **UK-5099**. Compounds with pyridyl substitution (**180, 184, 190** and **191**) also showed good inhibitory effect. Compound **190** with its 5-methyl-substituted-2-pyridyl substitution showed comparable inhibition as compound **231** (80.0 nM) and superior activity compared to the **UK-5099**. **Table 6** provides the IC_{50} values of compounds **176** to **191.**

Table 6: MCT1 inhibitory activity of indole-3-cyanoacrylate derivatives against A-549 cells in 3-BP assay

Compound code	A-549 (MCT1 inhibition) IC_{50} nm ± SD
176	314 ± 47 nM
177	287 ± 47 nM
178	112 ± 10 nM
179	193 ± 10 nM
180	198 ± 41 nM
181	135 ± 21 nM
182	105 ± 62 nM
183	196 ± 51 nM
184	81.0 ± 42 nM
185	109 ± 30 nM

186	105 ± 90 nM
187	109 ± 20 nM
188	793 ± 138 nM
189	214 ± 32 nM
190	82.3 ± 44 nM
191	109 ± 30 nM
UK-5099	0.17 ± 0.032 µM

6.4.1.3. Indazole based compounds linked with N-phenylpropanamide derivatives

Further we also evaluated indazole based compounds linked with N-phenylpropanamide derivatives for MCT1 inhibition against A-549 cells, results obtained from the study demonstrated that compounds bearing 4-phenylcarboxamide moiety linked with 4-methoxy **(200)** and 4-fluoro **(201)** phenylpropanamide linker showed stronger MCT1 inhibition than other compounds with IC_{50} value 4.34 ± 0.03 µM and 4.49 ± 0.13 µM respectively. However, 2-methyl **(198)** and 4-metyl **(199)** substituted linker compound slightly decreases the activity with IC_{50} value 6.76 ± 0.1 and 6.53 ± 0.16 µM respectively. compound with 4-fluoro group at 4^{th} position of the linker **(209)** also showed good to moderate MCT1 inhibition with IC_{50} value 7.45 ± 0.04 µM. compound possesses 4-chloro phenyl carboxamide moiety linked with phenyl **(207)** and 4-methyl **(208)** substituted linker also displayed remarkable MCT 1inhibition with IC_{50} value 11.1 ± 0.46 µM and 11.5 ± 0.25

µM. In short unsubstituted phenyl carboxamide moiety is more important for MCT1 inhibition than electron donating and electron withdrawing substituted phenyl carboxamide moiety. Nevertheless, all the compounds also showed acceptable MCT1 inhibition when compared with reference MCT1 inhibitor such as **UK-5099**. **Table 7** provides the IC_{50} values of all compounds.

Table 7: MCT1 inhibitory activity of indazole based compounds linked with N-phenyl propanamide derivatives against A-549 cells

Compound code	A-549 (MCT1 inhibition) IC_{50} ± SD
197	12.56 ± 0.63 µM
198	6.76 ± 0.1 µM
199	6.53 ± 0.16 µM
200	4.34 ± 0.03 µM
201	4.49 ± 0.13 µM
202	12 ± 0.2 µM
203	6.2 ± 0.11 µM
204	17.37 ± 0.61 µM
205	18.73 ± 1.63 µM
206	15.43 ± 0.42 µM
207	11.1 ± 0.46 µM
208	11.5 ± 0.25 µM
209	7.45 ± 0.04 µM
UK-5099	0.17 ± 0.032 µM

6.4.1.4. 3-phenyl indazole based compounds linked with N-phenylacetamide derivatives

Another set of 3-phenyl indazole based compounds linked with N-phenyl acetamide linker were also evaluated for MCT1 inhibition study by using 3-bromopyruvate assay. results obtained from this functional assay indicated that compound bearing 3 phenyl rings at 3rd position of the indazole and electron donating methyl group **(214)** at 2nd position of the acetamide liker demonstrated excellent MCT1 inhibition with IC_{50} value 5.8 ± 0.19 µM. Replacement of methyl group with electron withdrawing group (**216** and **217**) slightly

decreases the MCT1 inhibition with IC_{50} value 8.24 ± 0.02 µM and 7.81 ± 0.22 µM respectively. On the other hand, it has been observed that substitution on phenyl ring with sulfonyl moiety remarkably decreases the activity when compared with plane phenyl substituted compounds. Among all the compounds, compounds **218-222** displayed moderate to good MCT1 in inhibition with IC_{50} value fall in range between 7.81-16 µM. **Table 8** provides the IC_{50} values of all compounds.

Table 8: MCT1 inhibitory activity of 3-phenyl indazole based compounds linked with N-phenyl acetamide derivatives against A-549 cells

Compound code	A-549 (MCT1 inhibition) IC_{50} ± SEM
213	12 ± 0.31 µM
214	5.8 ± 0.19 µM
215	10.5 ± 0.21 µM
216	8.24 ± 0.02 µM
217	7.81 ± 0.22 µM
218	12.37 ± 0.03 µM
219	13.13 ± 0.15 µM
220	14.3 ± 0.06 µM
221	12.37 ± 0.24 µM
222	16.63 ± 0.26 µM
UK-5099	0.17 ± 0.032 µM

6.4.2. Intracellular pH measurement for MCT4

MCT4 is a key protein in the metabolic reprogramming of hypoxic tumor cells. MCT4 inhibition was assessed by using a pH-sensitive fluorescence dye BCECF-AM in the literature with minor modifications. In short, functional MCT4 inhibition prevents extrusion of acidic lactate which acidifies the cytosol of the MCT4-expressing cancer cells (MDA-MB-231). The degree of inhibition is reflected in the magnitude of pH reduction. Unfortunately, in the current study, none of the evaluated derivatives showed pH reduction in MCT4-expressing MDA-MB-231 cells

6.5. Cell cycle distribution analysis

In order to prove that indole derivatives impair cancer cell proliferation and to confirm their antiproliferative nature, we conducted a cell cycle distribution analysis *via* a propidium iodide (PI) flow cytometry assay as reported earlier. A-549 cells were exposed to the most potent MCT1 inhibitor, compound **184** (5 µM), and the distribution of the cells in the cell cycle phases sub-G_1, G_0/G_1, S, and G_2/M was calculated compared to untreated A-549 cells. The antineoplastic agent **Doxorubicin** (5 µM) was used as reference. **Figure 38** shows the histograms for untreated (A), compound **184**-treated (B), and **Doxorubicin** -treaded cells (C). Compound **184** caused a disruption of the cell cycle of A-549 cancer cells, indicated by a shift from the predominant G_0/G1 phase (**Figure 38 A**) to the apoptotic sub-G1 phase as well as the G_2/M phase (**Figure 38 B**). A similar G_2/M arrest could be observed for reference compound **doxorubicin** (**Figure 38 C**), however, MCT1 inhibitor **231** led to a larger fraction of cells into the sub-G1 phase, indicating induced apoptosis. This experiment discovered that compound **184** inhibits cell proliferation, causing cell cycle arrest and, eventually apoptosis. To confirm our findings, we conducted an apoptosis assay using compound **184**.

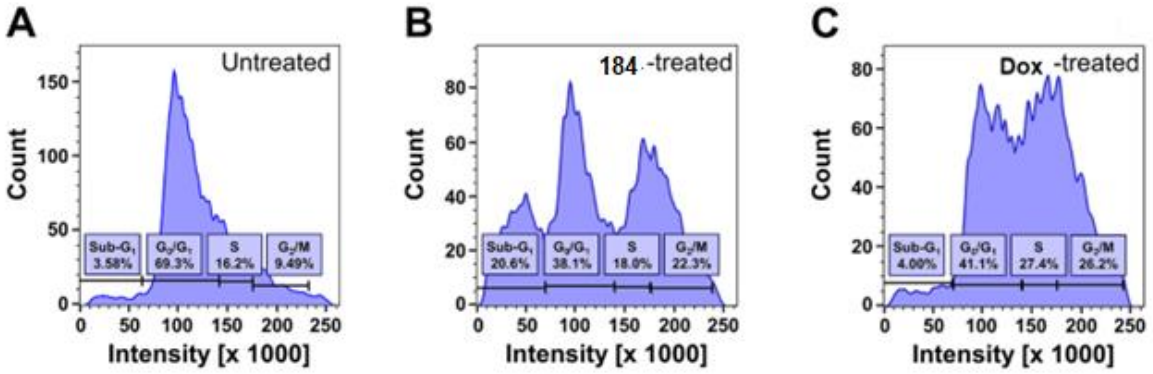

Figure 38: Distribution of cell cycle phases of (A): untreated A-549 cancer cells; (B): A-549 cells treated with compound **184** (5 µM); (C): **Doxorubicin** (5 µM).

6.6. Apoptosis assay

As compound **184** increased the sub-G_1 cell cycle fraction of A-549 cells, we investigated its capability to induce apoptosis in a PI/Annexin V-FITC staining assay as reported earlier. In short, cells that were stained with PI only were considered as necrotic cells (Q1), while cells stained with both PI and Annexin V were late apoptotic (Q2), and cells stained only with Annexin V were early apoptotic (Q4). Cells negative on both PI and Annexin V were considered as living cells (Q3). Compound **184** (5 µM) increased the percentage of total apoptotic cells by over a factor of 13 from 0.51% to 6.68% when compared to the untreated A-549 cells, indicating that **184** exhibited cytotoxicity against the A-549 cancer cells *via* inducing apoptosis. **Figure 39** shows the flow cytometry scatter plot of untreated (A) compared to compound **184**-treated A-549 cells (B).

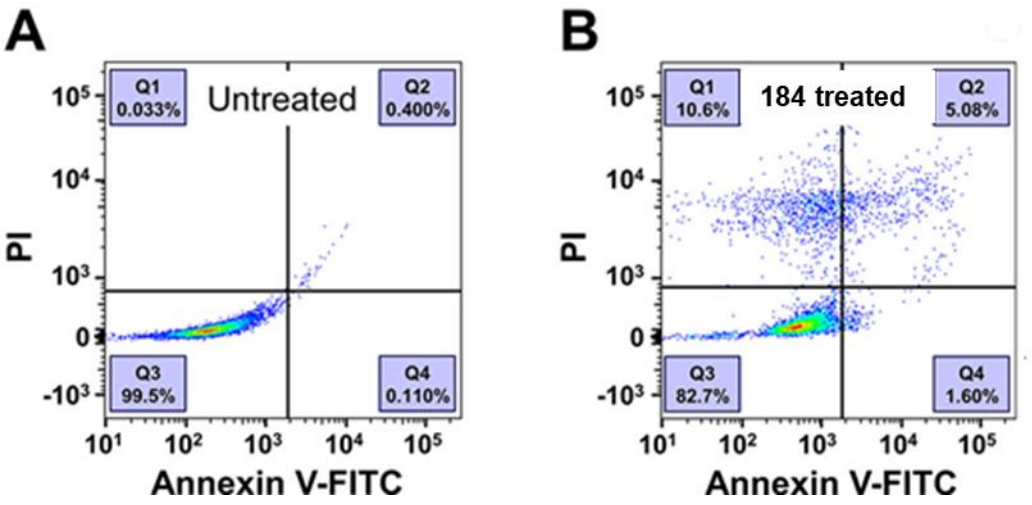

Figure 39: Distribution of apoptotic A-549 cancer cells when untreated (A) or exposed to compound **184** (B).

6.7. Efficacy Assays of compounds in combination with doxorubicin

MCT1 inhibition is expected to increase the efficacy of anticancer agents by disrupting the cancer cell energy supply. To test this hypothesis, we evaluated the effect of anticancer drug **doxorubicin** on MCT-1 overexpressing A-549 cells in combination with compounds **164**, **168,** and **200** at 0.5 µM, 1 µM and 5 µM concentration for a 72 hr by using MTT assay. Results obtained from the efficacy study indicated that three compounds **164**,**168,** and **200** sensitized the cells against **doxorubicin** and increases the effectiveness of **doxorubicin** by 1.35-fold ,1.48-fold and 1.53 respectively. As shown in **figure 40** there is shift of concentration response curve to the left, exhibiting their capability to increase susceptibility toward anticancer drug. **Table 9** provides the IC_{50} value of **doxorubicin** without or with increasing concentration of compound **164**,**168,** and **200.**

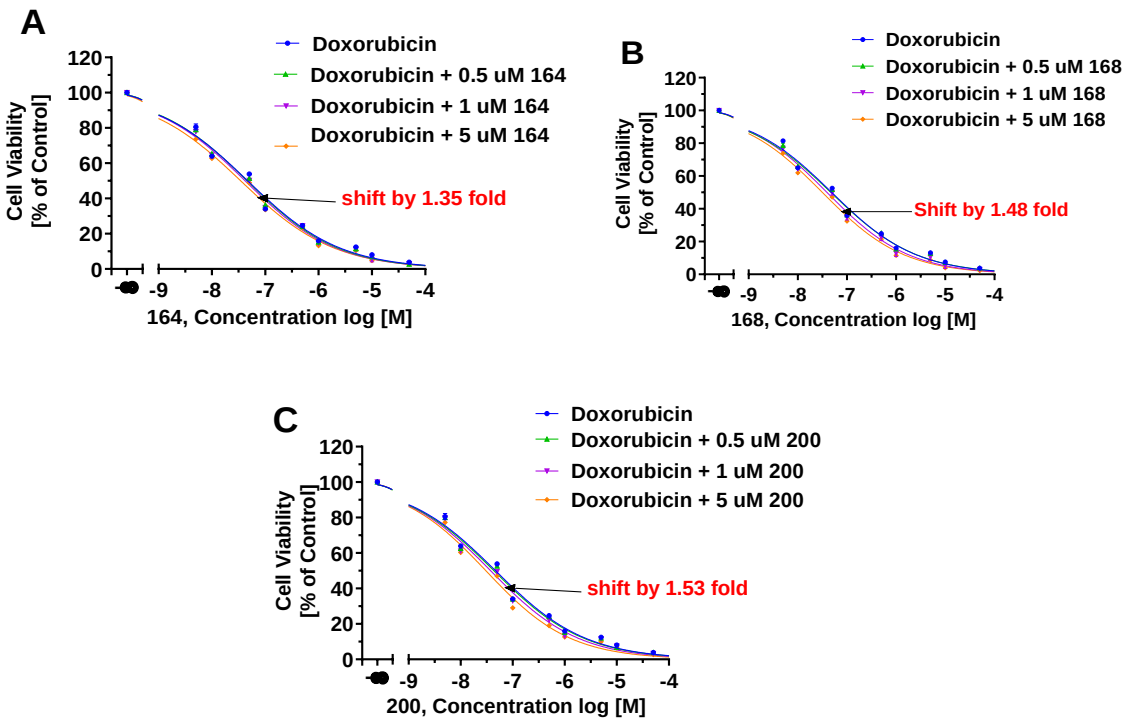

Figure 40: Efficacy study of indazole derivatives against A-549 cells

Table 9: IC_{50} value of **doxorubicin** without or with increasing concentration of compound 164,168 and 200

Compound code	Doxorubicin + 0 µM test compound	Doxorubicin + 0.5 µM test compound	Doxorubicin + 1 µM test compound	Doxorubicin + 5 µM test compound
164	46.72 ± 0.03 nM	45.59 ± 0.02 nM	41.94 ± 0.02 nM	34.59 ± 0.02 nM
168	46.72 ± 0.03 nM	46.85 ± 0.02 nM	39.14 ± 0.02 nM	31.55 ± 0.02 nM
200	46.72 ± 0.03 nM	45.99 ± 0.02 nM	41.99 ± 0.02 nM	34.59 ± 0.02 nM

Similarly compound **184** or **190** (50 nM, 100 nM, or 500 nM) were evaluated in combination with **doxorubicin. Figure 41** shows the resultant concentration effect curves of **doxorubicin** without and with supplementation of compounds **184** (A) or **190** (B). In both cases, the compounds sensitized the cells against **doxorubicin** by factors of 2.5

and 2.6, respectively, as indicated by the shift of the concentration-effect curve to the left, demonstrating their capability to increase susceptibility toward antineoplastic agents (**figure 41**). **Table 10** provides the IC_{50} value of **doxorubicin** without or with increasing concentration of compound **184** and **190.**

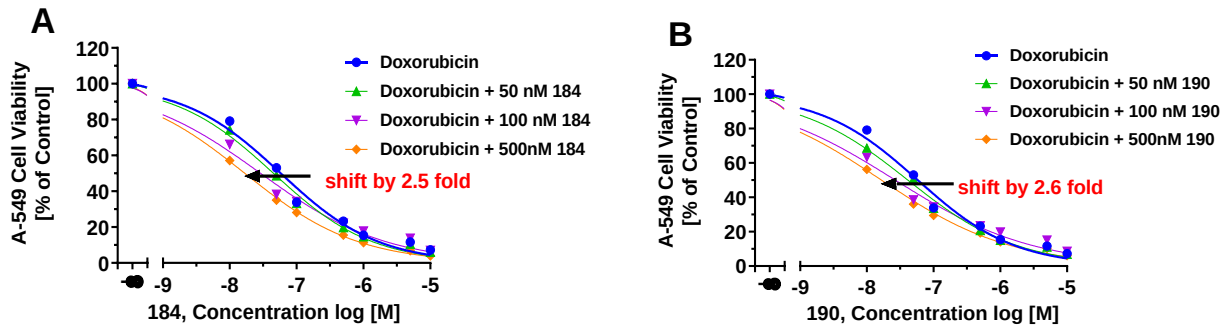

Figure 41: Efficacy study of indole derivatives against A-549 cells

Table 10: IC_{50} value of **doxorubicin** without or with increasing concentration of compound 231 and 237.

Compound code	Doxorubicin + 0 nM test compound	Doxorubicin + 50 nM test compound	Doxorubicin + 100 nM test compound	Doxorubicin + 500 nM test compound
184	47.6 ± 0.7 nM	40.0 ± 0.2 nM	27.7 ± 0.4 nM	19.4 ± 0.3 nM
190	47.6 ± 0.7 nM	38.6 ± 0.5 nM	25.4 ± 0.4 nM	18.6 ± 0.4 nM

6.8. Cell viability in presence and absence of glucose supplement

In order to prove cell death of MCT1-expressing cancer cells results from glucose deprivation, we conducted additional MTT-based cell viability experiments with compounds **184** and **190** supplementing glucose (25% and 50% of the original glucose concentration of 4.5 g/L every 12 hr) over the time span of 72 hr. In this study, we prove that supplementation of glucose prevents cell toxicity of the MCT1 inhibitors compound

184 (**Figure 42 A**) and **190** (**Figure 42 B**), and thus, confirming that glucose deprivation is the main cause of cell death mediated by MCT1 inhibitors.

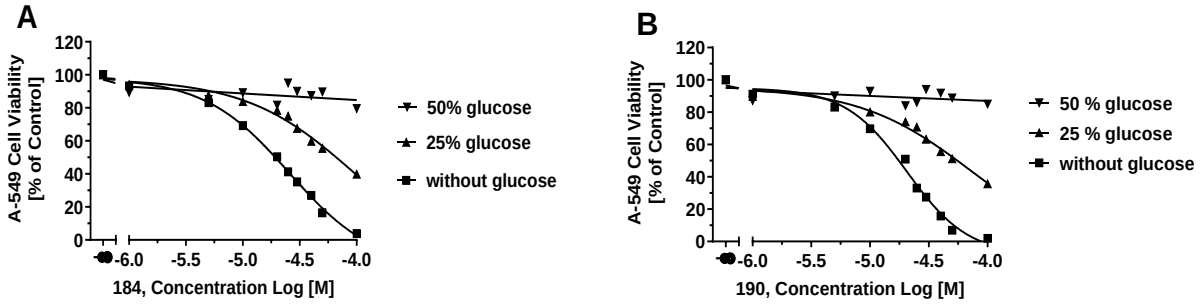

Figure 42: MTT-based cell viability assays of compound 184 (A) and 190(B) either without (●) or with 25% (▲) and 50% (▼) supplemented glucose every 12 hr over the time course of 72 hr.

7. Summary and Conclusion

In the current study we designed and synthesized a library of small molecules having potential target MCT1 and MCT4 based on the literature available. A total of 151 molecules were synthesized belonging to different scaffolds such as coumarins (11), flavonoids (09), quinazolinones (26), indole cyanoacrylate and cyanoacrylic acid derivatives linked with N-benzyl linker (12), indazole cyanoacrylic acid derivatives (7 molecules), indazole Schiff base (11), indazole-3-carboxamide (36), indole-3-cyanoacrylate(16), indazole based compounds linked with N-phenylpropanamide (13), and 3-phenylindazole based compounds linked with N-phenylacetamide (10). The synthesized molecules were characterized by using Mass, IR, ^{1}H NMR, and HPLC.

Biological investigation of the synthesized molecules were carried out by cytotoxicity assays and functional assays to determine anticancer potential. Initially, cytotoxicity of all synthesized compounds was evaluated against four tumor cell lines i.e, cervical (SiHa), breast (MDA-MB-231), breast (MCF-7), and lung (A-549) via MTT assay. Results

obtained for the initially screened molecules, which includes coumarin, flavonoids, quinazolinone and indazole Schiff based derivatives suggested that none of the compound exhibited sufficient MCT1 and MCT4 inhibition even at high concentration when compared with standard (**CHC** / **IND CHC**). In case coumarin derivatives only 3 compounds (**10,11** and **12**) showed some cytotoxicity against cervical cells in low glucose media, similar molecules did not exhibit any potential inhibition in high glucose media. Hence, we designed new sets of target molecules bearing indole and indazole scaffolds with varying substitution at N1 and 3rd position of indole and indazole.

In the case of indazole-3-carboxamide compounds linked with N-phenylacetamide derivatives, compound **167**, **152** and **137** turned out to be the most cytotoxic towards A-549, MDA-MB-231 and MCF-7 cells. In another set of series indole-3-cyanoacrylate derivatives linked with N-phenylacetamide derivatives, compounds **178**, **190** and **180** showed promising inhibitory activity towards A-549, MDA-MB-231 and MCF-7cells respectively. Inspired by the results obtained from previous study, we functionalized the indazole moiety by retaining the carboxamide moiety at 3rd position of the indazole and replacing N1 position with N-phenylpropanamide linker. Here we found that compound **202, 200**, and **206** showed good inhibitory effect against the A-549, MCF-7 and MDA-MB-231 cells respectively. In the last set of indazole based molecules, we carried out modification in indazole scaffold by replacing the 3-carboxamide moiety with 3-aryl group, while keeping the N-phenylcetamide linker same. Compounds **216, 222** and **220** displayed the strongest antiproliferative activity against MCT1 overexpressing A-549, MCF-7 and MDA-MB-231 cells. All these molecules when screened against NIH/3T3 cells showed no cytotoxic effect against these non-cancer fibroblast cells. This suggests

selectivity of cells toward cancer cells over non-cancer cells and potential non-toxicity against healthy cells.

Further, the inhibitory activity of indazole and indole-based derivatives against MCT1 was determined by using 3-bromopyruvate (3-BP) functional assay in A-549 cells. The results obtained from the study suggested that all indazole carboxamide or 3-aryl indazole derivatives (**161, 200** and **214**), indole-3-cyanoacrylate derivatives (**184**) possess high inhibitory potential in sub-micromolar to nanomolar concentration ranges. MCT4 inhibition was further assessed by using a pH-sensitive fluorescence dye BCECF-AM in MCT4 overexpressing MDA-MB-231 cells, However, none of the evaluated derivatives showed pH reduction in MCT4-expressing MDA-MB-231 cells suggesting no effect against MCT4. In order to prove that synthesized compounds impair cancer cell proliferation and to confirm their antiproliferative nature, we conducted a cell cycle distribution analysis via a propidium iodide (PI) flow cytometry assay as reported earlier. A-549 cells were exposed to the most potent MCT1 inhibitor, compound **185** and the distribution of the cells in the cell cycle phases sub-G1, G0/G1, S, and G2/M was calculated compared to untreated A-549 cells. Compound **185** caused a disruption of the cell cycle of A-549 cancer cells, indicated by a shift from the predominant G0/G1 phase to the apoptotic sub-G1 phase as well as the G2/M phase, led to induced apoptosis. This experiment showed that compound **185** inhibits cell proliferation, causing cell cycle arrest and, eventually apoptosis.

MCT1 inhibition is expected to increase the efficacy of anticancer agents by disrupting the cancer cell energy supply. To test this hypothesis, we evaluated the effect of anticancer drug **doxorubicin** on MCT-1 overexpressing A-549 cells in combination with

compounds **164, 168** and **200** at 0.5 µM, 1 µM and 5 µM concentration whereas **184** and **190** at 50 nM, 100 nM, and 500 nM concentration for a 72 hr by using MTT assay. Results obtained from the efficacy study indicated that these compounds **164, 168, 184, 190** and **200** sensitized the cells against **doxorubicin** and increased the effectiveness of **doxorubicin** by 1.35-fold ,1.48-fold, 2.5-fold, 2.6-fold and 1.53 respectively.

Finally, we performed additional experiments using most potent MCT1 inhibitors **184** and **190** to prove that antiproliferative effect is due to the forced glucose consumption resulting from blockage of lactate influx and resulting insufficient glucose availability. Here, we conducted MTT-based cell viability experiments with compounds **184** and **190** supplementing additional glucose every 6 hr for total study duration of 72 hr. In this study, we found that supplementation of glucose prevents cell toxicity of the MCT1 inhibitors (**184** and **190**) in comparison to one not supplemented with additional glucose. This confirms that glucose deprivation is the main cause of cell death mediated by MCT1 inhibitors. Owing to the importance of MCTs in tumor metabolism in several cancers, we believe that these inhibitors have good potential to be developed as broad-spectrum anticancer agents.

8. Future perspective

In the current research work we could identify several potent and non-toxic MCT1 inhibitors belonging to the indole and indazole scaffolds. These molecules have a great potential for further optimisation to identify newer cancer therapeutics targeting monocarboxylate transporters. Current work sets the groundwork for following possibilities that could be explored in future study.

Some of these leads include:

1) Enhancing the effectiveness and other relevant physical and chemical properties of the identified hits through further optimization, therefore improving their potency in drug action.

2) Optimisation of lead molecules to improve the ADMET profile

3) Additionally, the optimized lead molecules could be investigated further to assess their *in vivo* efficacy.

9. References

[1] R.L. Siegel, K.D. Miller, H.E. Fuchs, A. Jemal, Cancer statistics, 2022, CA: A Cancer Journal for Clinicians. 72 (2022) 7–33. https://doi.org/10.3322/caac.21708.

[2] D. Loomis, W. Huang, G. Chen, The International Agency for Research on Cancer (IARC) evaluation of the carcinogenicity of outdoor air pollution: focus on China, Chin J Cancer. 33 (2014) 189–196. https://doi.org/10.5732/cjc.014.10028.

[3] G. Housman, S. Byler, S. Heerboth, K. Lapinska, M. Longacre, N. Snyder, S. Sarkar, Drug Resistance in Cancer: An Overview, Cancers (Basel). 6 (2014) 1769–1792. https://doi.org/10.3390/cancers6031769.

[4] B. Jiang, Aerobic glycolysis and high level of lactate in cancer metabolism and microenvironment, Genes & Diseases. 4 (2017) 25–27. https://doi.org/10.1016/j.gendis.2017.02.003.

[5] M.G. Vander Heiden, L.C. Cantley, C.B. Thompson, Understanding the Warburg Effect: The Metabolic Requirements of Cell Proliferation, Science. 324 (2009) 1029–1033. https://doi.org/10.1126/science.1160809.

[6] A.L. Harris, Hypoxia--a key regulatory factor in tumour growth, Nat Rev Cancer. 2 (2002) 38–47. https://doi.org/10.1038/nrc704.

[7] F. Végran, R. Boidot, C. Michiels, P. Sonveaux, O. Feron, Lactate influx through the endothelial cell monocarboxylate transporter MCT1 supports an NF-κB/IL-8 pathway that drives tumor angiogenesis, Cancer Res. 71 (2011) 2550–2560. https://doi.org/10.1158/0008-5472.CAN-10-2828.

[8] A.P. Halestrap, The SLC16 gene family – Structure, role and regulation in health and disease, Molecular Aspects of Medicine. 34 (2013) 337–349. https://doi.org/10.1016/j.mam.2012.05.003.

[9] P.C. McDonald, S.C. Chafe, S. Dedhar, Overcoming Hypoxia-Mediated Tumor Progression: Combinatorial Approaches Targeting pH Regulation, Angiogenesis and Immune Dysfunction, Front Cell Dev Biol. 4 (2016) 27. https://doi.org/10.3389/fcell.2016.00027.

[10] P.H. Boasquevisque, V. Schoeneberger, L. Caporiccio, R. Vellanki, M. Koritzinsky, B.G. Wouters, Inhibiting lactate transporters MCT-1 and MCT-4 target hypoxic HNSCC cells and sensitize them to metformin, Cancer Research. 78 (2018) 5476. https://doi.org/10.1158/1538-7445.AM2018-5476.

[11] T. Todenhöfer, R. Seiler, C. Stewart, I. Moskalev, J. Gao, S. Ladhar, A. Kamjabi, N. Al Nakouzi, T. Hayashi, S. Choi, Y. Wang, S. Frees, M. Daugaard, H.Z. Oo, P. Fisel, M. Schwab, E. Schaeffeler, J. Douglas, J. Hennenlotter, J. Bedke, E.A. Gibb, L. Fazli, A. Stenzl, P.C. Black, Selective Inhibition of the Lactate Transporter MCT4 Reduces Growth of Invasive Bladder Cancer, Molecular Cancer Therapeutics. 17 (2018) 2746–2755. https://doi.org/10.1158/1535-7163.MCT-18-0107.

[12] H. Lu, R.A. Forbes, A. Verma, Hypoxia-inducible Factor 1 Activation by Aerobic Glycolysis Implicates the Warburg Effect in Carcinogenesis*, Journal of Biological Chemistry. 277 (2002) 23111–23115. https://doi.org/10.1074/jbc.M202487200.

[13] A.P. Halestrap, N.T. Price, The proton-linked monocarboxylate transporter (MCT) family: structure, function and regulation., Biochem J. 343 (1999) 281–299.

[14] A.P. Halestrap, M.C. Wilson, The monocarboxylate transporter family—Role and regulation, IUBMB Life. 64 (2012) 109–119. https://doi.org/10.1002/iub.572.

[15] A.P. Halestrap, The monocarboxylate transporter family--Structure and functional characterization, IUBMB Life. 64 (2012) 1–9. https://doi.org/10.1002/iub.573.

[16] A.P. Halestrap, The SLC16 gene family - structure, role and regulation in health and disease, Mol Aspects Med. 34 (2013) 337–349. https://doi.org/10.1016/j.mam.2012.05.003.

[17] C. Pinheiro, E.A. Garcia, F. Morais-Santos, C. Scapulatempo-Neto, A. Mafra, R.D. Steenbergen, E. Boccardo, L.L. Villa, F. Baltazar, A. Longatto-Filho, Lactate

transporters and vascular factors in HPV-induced squamous cell carcinoma of the uterine cervix, BMC Cancer. 14 (2014) 751. https://doi.org/10.1186/1471-2407-14-751.

[18] N. Draoui, O. Feron, Lactate shuttles at a glance: from physiological paradigms to anti-cancer treatments, Dis Model Mech. 4 (2011) 727–732. https://doi.org/10.1242/dmm.007724.

[19] S.K. Parks, J. Chiche, J. Pouysségur, Disrupting proton dynamics and energy metabolism for cancer therapy, Nat Rev Cancer. 13 (2013) 611–623. https://doi.org/10.1038/nrc3579.

[20] S. Puri, K. Juvale, Monocarboxylate transporter 1 and 4 inhibitors as potential therapeutics for treating solid tumours: A review with structure-activity relationship insights, Eur. J. Med. Chem. 199 (2020) 112393. https://doi.org/10.1016/j.ejmech.2020.112393.

[21] S. Puri, K. Stefan, S.L. Khan, J. Pahnke, S.M. Stefan, K. Juvale, Indole Derivatives as New Structure Class of Potent and Antiproliferative Inhibitors of Monocarboxylate Transporter 1 (MCT1; SLC16A1), J. Med. Chem. 66 (2023) 657–676. https://doi.org/10.1021/acs.jmedchem.2c01612.

[22] A.P. Halestrap, R.M. Denton, Specific inhibition of pyruvate transport in rat liver mitochondria and human erythrocytes by alpha-cyano-4-hydroxycinnamate, Biochem J. 138 (1974) 313–316. https://doi.org/10.1042/bj1380313.

[23] C.-K. Shim, E.-P. Cheon, K.W. Kang, K.-S. Seo, H.-K. Han, Inhibition effect of flavonoids on monocarboxylate transporter 1 (MCT1) in Caco-2 cells, J Pharm Pharmacol. 59 (2007) 1515–1519. https://doi.org/10.1211/jpp.59.11.0008.

[24] K.Y. Hu, D.G. Wang, P.F. Liu, Y.W. Cao, Y.H. Wang, X.C. Yang, C.X. Hu, L.J. Sun, H.T. Niu, Targeting of MCT1 and PFKFB3 influences cell proliferation and apoptosis in bladder cancer by altering the tumor microenvironment, Oncology Reports. 36 (2016) 945–951. https://doi.org/10.3892/or.2016.4884.

[25] R. Polański, C.L. Hodgkinson, A. Fusi, D. Nonaka, L. Priest, P. Kelly, F. Trapani, P.W. Bishop, A. White, S.E. Critchlow, P.D. Smith, F. Blackhall, C. Dive, C.J. Morrow, Activity of the monocarboxylate transporter 1 inhibitor AZD3965 in small cell lung cancer, Clin Cancer Res. 20 (2014) 926–937. https://doi.org/10.1158/1078-0432.CCR-13-2270.

[26] R. Lamb, H. Harrison, J. Hulit, D.L. Smith, M.P. Lisanti, F. Sotgia, Mitochondria as new therapeutic targets for eradicating cancer stem cells: Quantitative proteomics and functional validation via MCT1/2 inhibition, Oncotarget. 5 (2014) 11029–11037. https://doi.org/10.18632/oncotarget.2789.

[27] N. Draoui, O. Schicke, A. Fernandes, X. Drozak, F. Nahra, A. Dumont, J. Douxfils, E. Hermans, J.-M. Dogné, R. Corbau, A. Marchand, P. Chaltin, P. Sonveaux, O. Feron, O. Riant, Synthesis and pharmacological evaluation of carboxycoumarins as a new antitumor treatment targeting lactate transport in cancer cells, Bioorganic & Medicinal Chemistry. 21 (2013) 7107–7117. https://doi.org/10.1016/j.bmc.2013.09.010.

[28] J.Y. Lee, I. Lee, W.J. Chang, S.M. Ahn, S.H. Lim, H.S. Kim, K.H. Yoo, K.S. Jung, H.-N. Song, J.H. Cho, S.Y. Kim, K.-M. Kim, S. Lee, S.T. Kim, S.H. Park, J. Lee, J.O. Park, Y.S. Park, H.Y. Lim, W.K. Kang, MCT4 as a potential therapeutic target for metastatic gastric cancer with peritoneal carcinomatosis, Oncotarget. 7 (2016) 43492–43503. https://doi.org/10.18632/oncotarget.9523.

[29] S.Y.C. Choi, H. Xue, R. Wu, L. Fazli, D. Lin, C.C. Collins, M.E. Gleave, P.W. Gout, Y. Wang, The MCT4 Gene: A Novel, Potential Target for Therapy of Advanced Prostate Cancer, Clin Cancer Res. 22 (2016) 2721–2733. https://doi.org/10.1158/1078-0432.CCR-15-1624.

[30] S. Puri, I. Ahmad, H. Patel, K. Kumar, K. Juvale, Evaluation of oxindole derivatives as a potential anticancer agent against breast carcinoma cells: In vitro, in silico, and molecular docking study, Toxicol In Vitro. 86 (2023) 105517. https://doi.org/10.1016/j.tiv.2022.105517.

[31] V.P. Sandanayaka, S. Shechter, S. Shacham, D. Mccauley, E. Baloglu, Nuclear transport modulators and uses thereof, WO2013170068A3, 2014. https://patents.google.com/patent/WO2013170068A3/en (accessed May 22, 2023).

[32] C. Roberts, Y. Zhang, F. BEAUMIER, L. LEPISSIER, J.J. MARINEAU, P.B. Rahl, K. Sprott, S. CIBLAT, B. SOW, R. LAROUCHE-GAUTHER, L. BERSTLER, Compounds for the modulation of myc activity, WO2016196910A1, 2016. https://patents.google.com/patent/WO2016196910A1/en (accessed May 22, 2023).

[33] F. Crestey, S. Stiebing, R. Legay, V. Collot, S. Rault, Design and synthesis of a new indazole library: direct conversion of N-methoxy-N-methylamides (Weinreb amides) to 3-keto and 3-formylindazoles, Tetrahedron. 63 (2007) 419–428. https://doi.org/10.1016/j.tet.2006.10.063.

[34] P.F. Lamie, W.A.M. Ali, V. Bazgier, L. Rárová, Novel N-substituted indole Schiff bases as dual inhibitors of cyclooxygenase-2 and 5-lipoxygenase enzymes: Synthesis, biological activities in vitro and docking study, European Journal of Medicinal Chemistry. 123 (2016) 803–813. https://doi.org/10.1016/j.ejmech.2016.08.013.

[35] S.H. Henderson, R.A. West, S.E. Ward, M.A. Honey, Metal-free selective mono-halodecarboxylation of heteroarenes under mild conditions, Royal Society Open Science. 5 (2018) 180333. https://doi.org/10.1098/rsos.180333.

[36] A. Ben-Yahia, M. Naas, N.E. Brahmi, S.E. Kazzouli, J.-P. Majoral, E.M. Essassi, G. Guillaumet, Microwave-assisted Suzuki-Miyaura Cross-Coupling of Free (NH) 3-Bromoindazoles, Current Organic Chemistry. 17 (n.d.) 304–309.

Submitted by:

Candidate: Mr. Sachin Puri **Supervisor: Dr. Kapil Juvale**